

EFFECT OF SPHERODIZING ON MACHINABILITY CHARACTERISTICS
AND MICROSTRUCTURE OF MEDIUM CARBON STEELS

A THESIS SUBMITTED TO
THE GRADUATE SCHOOL OF NATURAL AND APPLIED SCIENCES
OF
MIDDLE EAST TECHNICAL UNIVERSITY

BY

EMRE YANARDAĞ

IN PARTIAL FULFILLMENT OF THE REQUIREMENTS
FOR
THE DEGREE OF MASTER OF SCIENCE

IN
MECHANICAL ENGINEERING

AUGUST 2004

Approval of the Graduate School of Natural And Applied Sciences

Prof. Dr. Canan ÖZGEN
Director

I certify that this thesis satisfies all the requirements as a thesis for the degree of Master of Science.

Prof. Dr. Kemal İDER
Head of Department

This is to certify that I have read this thesis and that in my opinion it is fully adequate, in scope and quality, as a thesis for the degree of Master of Science.

Assoc. Prof. Dr. C. Hakan GÜR
Co-Supervisor

Prof.Dr.A.Bülent DOYUM
Supervisor

Examining Committee Members:

Prof. Dr.R.Orhan YILDIRIM (METU, ME) _____

Prof.Dr.A.Bülent DOYUM (METU, ME) _____

Assoc.Prof. Dr.C. Hakan GÜR (METU, METE) _____

Prof. Dr. Levent PARNAS (METU, ME) _____

Asst. Prof. Dr. Serkan DAĞ (METU, ME) _____

I hereby declare that all information in this document has been obtained and presented in accordance with academic rules and ethical conduct. I also declare that, as required by these rules and conduct, I have fully cited and referenced all material and results that are not original to this work.

Name, Last Name: Emre YANARDAĞ

Signature :

ABSTRACT

EFFECT OF SPHERODIZING ON MACHINABILITY CHARACTERISTICS AND MICROSTRUCTURE OF MEDIUM CARBON STEELS

Yanardağ, Emre

M.S., Department of Mechanical Engineering

Supervisor: Prof. Dr.A.Bülent DOYUM

Co-Supervisor: Assoc.Prof.Dr. C.Hakan GÜR

August 2004, 115 pages

This study includes examination of the machinability characteristics of two medium carbon steel types (SAE 1040 and SAE 1050) as a result of spherodizing treatment. Both steel types were handled into four categories according to their spherodizing treatment parameters (temperature and time). Microstructural investigation, hardness and ultrasonic sound velocity measurement (with both longitudinal and transverse waves) of these steels were performed, and effect of applied heat treatments on microstructure, hardness and ultrasonic sound velocity was investigated. Pulse-echo method has been used for ultrasonic sound velocity measurements, and measurements were performed with 5 and 10 MHz longitudinal and 5 MHz transverse wave probes. Tool life criterion was used for determining the machinability characteristics of the steels. For this purpose, flank wear land measurements were performed on the cutting tools. Results have showed that, by applying heat treatment it is possible to change the microstructure, hardness, ultrasonic sound velocity and machinability characteristics of a steel.

Keywords: Machinability, tool life, flank wear, ultrasonic velocity, spherodizing, heat treatment, hardness, microstructure

ÖZ

KÜRESELLEŞTİRMENİN ORTA KARBONLU ÇELİKLERİN İŞLENEBİLİRLİK ÖZELLİKLERİ VE MİKROYAPISINA ETKİSİ

Yanardağ, Emre

Yüksek Lisans, Makina Mühendisliği Bölümü

Tez Yöneticisi: Prof. Dr.A.Bülent DOYUM

Ortak Tez Yöneticisi : Doç.Dr. C.Hakan GÜR

Ağustos 2004, 115 sayfa

Bu çalışma, iki tip orta karbonlu çeliğin (SAE 1040 ve SAE 1050) küreselleştirme işlemi sonucu işlenebilirlik karakteristiklerinin değişiminin incelenmesini içermektedir. Her iki çelik tipi küreselleştirme işlemi parametrelerine (sıcaklık ve süre) göre dört gruba ayrılmıştır. Çelikler üzerinde mikroyapı incelemesi, sertlik ve ultrasonik ses hızı ölçümü (enine ve boyuna dalgalarla) gerçekleştirilmiş, ve uygulanan ısıtma işlemlerinin mikroyapı, sertlik ve ultrasonik ses hızı üzerindeki etkisi incelenmiştir. Ultrasonik ses hızı ölçümlerinde darbe-yankı metodu kullanılmış ve ölçümler 5 ve 10 MHz boyuna ile 5 MHz enine dalga probları ile yapılmıştır. Çeliklerin işlenebilirlik özelliklerinin incelenmesinde kalem ömrü kriteri kullanılmıştır. Bu amaçla, kesici kalemler üzerinde yan yüzey aşınma ölçümleri gerçekleştirilmiştir. Sonuçlar şunu göstermektedir ki, ısıtma işlemi uygulanarak çeliğin mikroyapı, sertlik, ultrasonik ses hızı ve işlenebilirlik özellikleri değiştirilebilmektedir.

Anahtar Kelimeler: İşlenebilirlik, kalem ömrü, yan yüzey aşınması, küreselleştirme, ısıtma işlemi, sertlik, mikroyapı

ACKNOWLEDGEMENTS

I wish to express my deepest gratitude to my family for their endless support and patience during this thesis, as throughout my whole education.

I am very grateful to my supervisor Prof.Dr. A.Bülent DOYUM and my co-supervisor Assoc.Prof.Dr. C.Hakan GÜR for their encouragement and guidance since from the beginning, and for their open-minded point of view, which made this project possible.

I would like to express my sincere thanks to Mrs. Birnur DOYUM, and Mr. Orkun TUNCER for their great help during ultrasonic measurements.

I would also like to express my sincere thanks to Mr. Özdemir DİNÇ, Mr.Hüseyin ÇOLAK, Mr. Yusuf PAPUR, Mr.Haydar BOZKURT and Mr. Yusuf BAŞIBÜYÜK for their valuable help during the thesis studies.

TABLE OF CONTENTS

PLAGISARIM.....	iii
ABSTRACT	iv
ÖZ.....	v
ACKNOWLEDGEMENTS	vi
TABLE OF CONTENTS.....	vii
CHAPTER	
1. INTRODUCTION	1
1.1. Machining of Steels.....	1
1.2. Material Characterization by Non-Destructive Testing Methods.....	3
1.3. Aim of the Study	4
2. HISTORICAL BACKGROUND	6
3. CONCEPT OF MACHINABILITY	15
3.1. Measures of Machinability	15
3.2. Tool Life and Tool Wear.....	19
3.2.1 Wear and Wear Mechanisms.....	19
3.2.2 Forms of Wear in Metal Cutting	20
3.2.2.1 Crater Wear.....	21
3.2.2.2 Flank Wear.....	22
3.2.3 Tool Wear Measurement.....	24
3.2.4 Tool Wear and Time Relation.....	26
3.2.5 Determination of Tool Life	27

3.3. Turning Operation	28
3.4. Chip Formation	29
3.5. Cutting Tools	32
4. FACTORS AFFECTING MACHINABILITY OF STEELS.....	35
4.1. Chemical Composition	35
4.2. Hardness	36
4.3. Microstructure.....	38
4.4. Heat Treatment of Steels	40
4.4.1 Annealing.....	42
4.4.2 Spherodizing.....	46
5. SOUND VELOCITY	48
5.1. Introduction.....	48
5.2. Sound Velocity.....	49
5.3. Sound Velocity Measurement by Pulse-Echo System	54
6. EXPERIMENTAL PROCEDURE	56
6.1. Workpiece Characteristics	56
6.2. Flow-chart of the Study	58
6.3. Preliminary Studies	59
6.4. Heat Treatment of the Workpieces.....	59
6.5. Metallographic Analysis of the Workpieces.....	62
6.6. Hardness Test of the Workpieces.....	64
6.7. Ultrasonic Velocity Measurement of the Workpieces	65
6.8. Machinability Testing.....	66
6.8.1. Specification of the Engine Lathe.....	66

6.8.2. Specification of the Workpieces.....	67
6.8.3. Specification of the Cutting Tool.....	67
6.8.4. Cutting Operations.....	68
6.8.4.1 Preliminary Studies.....	68
6.8.4.2 Cutting Parameters.....	68
6.8.4.3 Tool Wear Measurement.....	69
7. RESULTS AND DISCUSSION.....	71
7.1. Introduction.....	71
7.2. Photomicrographs of the Workpieces	71
7.3. Results of the Hardness Measurements of the Workpieces.....	76
7.4. Results of the Ultrasonic Wave Velocity Measurements	80
7.5. Results of the Tool Life Tests.....	97
7.6. Discussion.....	103
8. CONCLUSION.....	107
REFERENCES.....	110

LIST OF SYMBOLS

V_{60}	: Cutting speed for a 60-minute tool life
A_1	: Constant
l	: Characteristic length
B.H.N	: Brinell hardness number of the work material
A_r	: Percent area reduction ratio of work material in tension
P	: Power
F_T	: Cutting force
f	: Feed
d	: Depth of cut
V	: Cutting speed
T	: Tool life
C, n	: Empirical constants
κ	: Bulk stiffness modulus
ρ	: Density
E	: Young's modulus
ν	: Poisson's ratio
G	: Shear modulus
c	: Sound velocity
f	: Frequency
λ	: Wavelength
T	: Period
t_s	: Measured time
d_f	: Work diameter
rpm	: Spindle speed

LIST OF TABLES

4.1	Machinability Effect of Alloying Elements	36
4.2	Optimum microstructures for best machinability ratings.....	39
5.1	Ultrasonic velocities in various media	54
6.1	Chemical composition analysis of the workpieces	56
6.2	Average mechanical properties of the workpieces	57
6.3	Approximate critical temperatures for workpieces	60
6.4	Summary of applied heat treatments.....	62
6.5	Necessary tool angles for standard tool life test	67
6.6	Cutting parameters used in tool life tests	68
6.7	Cutting velocities for different workpiece diameter at 285 rpm spindle speed	69
7.1	Numbers representing corresponding heat treatments	77
7.2	Hardness values of SAE 1040 workpieces.....	77
7.3	Hardness values of SAE 1050 workpieces.....	78
7.4	Ultrasonic wave velocities of SAE 1040 specimens (measured with 5 MHz longitudinal probe).....	80
7.5	Ultrasonic wave velocities of SAE 1050 specimens (measured with 5 MHz longitudinal probe).....	81

7.6	Ultrasonic wave velocities of SAE 1040 specimens (measured with 10 MHz longitudinal probe).....	85
7.7	Ultrasonic wave velocities of SAE 1050 specimens (measured with 10 MHz longitudinal probe).....	86
7.8	Ultrasonic wave velocities of SAE 1040 specimens (measured with 5 MHz transverse probe).....	90
7.9	Ultrasonic wave velocities of SAE 1050 specimens (measured with 5 MHz transverse probe).....	91
7.10	Flank wear measurement results of the SAE 1040 specimens	97
7.11	Flank wear measurement results of the SAE 1050 specimens	100

LIST OF FIGURES

3.1	Regions of tool wear in metal cutting	21
3.2	Crater wear on an indexible insert	22
3.3	Flank wear on an indexible insert	23
3.4	Some features of single-point tool wear in turning operations.....	25
3.5	Typical relationship between flank wear and cutting time	27
3.6	Typical relationship between tool life and cutting speed	28
3.7	Illustration of the turning operation	29
3.8	Discontinuous chip.....	30
3.9	Continuous chip.....	31
3.10	Continuous chip with built-up edge.....	32
3.11	Illustration of cutting tool rake and clearance angles	33
4.1	Effect of hardness on machinability.....	37
4.2	Iron-Carbon Phase Diagram	40
4.3	A Typical TTT Diagram for Plain Carbon Steels.....	42
4.4	Fe-Fe ₃ C phase diagram showing the temperature range of interest	43
5.1	Longitudinal wave.....	50
5.2	Transverse wave.....	51
5.3	Surface wave on steel.....	51
6.1	Top-view of the cutted specimen.....	63
6.2	Illustration of the ultrasonic wave travel.....	66

7.1	Photomicrographs of SAE 1040 specimens (with x100 magnification)	72
7.2	Photomicrographs of SAE 1050 specimens (with x100 magnification)	73
7.3	Photomicrographs of SAE 1040 specimens (with x500 magnification)	74
7.4	Photomicrographs of SAE 1050 specimens (with x500 magnification)	75
7.5	Hardness value changes of SAE 1040 and SAE 1050 specimens as a result of applied heat treatments	79
7.6	Sound velocity results of SAE 1040 and SAE 1050 specimens (measured with 5 MHz straight beam probe)	83
7.7	Hardness vs. sound velocity results of specimens (measured with 5 MHz straight beam probe)	84
7.8	Sound velocity results of SAE 1040 and SAE 1050 specimens (measured with 10 MHz longitudinal probe)	88
7.9	Hardness vs. sound velocity results of specimens (measured with 10 MHz straight beam probe)	89
7.10	Sound velocity results of SAE 1040 and SAE 1050 specimens (measured with 5 MHz shear wave probe).....	93
7.11	Hardness vs. sound velocity results of specimens (measured with 5 MHz shear wave probe).....	94
7.12	Comparison of velocity measurements of SAE 1040 steels with 5MHz and 10 MHz straight beam probes	95
7.13	Comparison of velocity measurements of SAE 1050 steel with 5MHz and 10 MHz straight beam probes.....	96

7.14	Flank wear land measurements of SAE 1040 specimens for cutting velocity $V=53.72$ m/min.....	98
7.15	Flank wear land measurements of SAE 1040 specimens for cutting velocity $V=65.36$ m/min.....	98
7.16	Tool life vs. cutting velocity curves for SAE 1040 specimens	99
7.17	Flank wear land measurements of SAE 1050 specimens for cutting velocity $V=53.72$ m/min.....	100
7.18	Flank wear land measurements of SAE 1050 specimens for cutting velocity $V=65.36$ m/min.....	101
7.19	Tool life vs. cutting velocity curves for SAE 1050 specimens	101
7.20	Change of tool lives of specimens at $V=53.72$ m/min cutting velocity as a function of hardness	102
7.21	Change of tool lives of specimens at $V=53.72$ m/min cutting velocity as a function of sound velocity	103

CHAPTER I

INTRODUCTION

1.1 Machining of Steels

In today's industry, there is a great requirement for steels to be machined in the desired shape, dimension or surface quality. Mostly used machining operations are turning, milling, boring, drilling and sawing. In terms of production economics, machining requires additional costs and it is very important that machining operations need to be done very efficiently in order to keep these expenditures at the level as low as possible.

When steels are machined into the desired shape, surface quality is needed to be good. A smooth surface is desired thus surface quality affects mechanical properties of steel. As well as surface quality, it is necessary that under definite cutting conditions, number of machined steel part having desired quality is needed to be as much as possible. By taking this considerations into account, a concept of machinability is needed to be discussed.

Machinability is a general term used to indicate that how easily a material can be machined to the size, shape and desired surface finish. The term machinability is often applied to work materials to describe their machining properties; it can have several meanings depending on the cutting process under consideration.

According to Boothroyd [1], when it is stated that material A is more machinable than material B, this can mean that a lower tool-wear rate is obtained with material A, or a better surface finish can be achieved with material A, or that less power is

required to machine material A. Since these parameters for assessing machinability are subject to numerous variables such as tool material and geometry, cutting conditions, and so forth, it is not surprising that machinability is a difficult concept to reduce to quantitative terms. The search for this material property which would indicate how machinable a material is, has eluded investigators for years. Thus, a simple and accurate definition of this property has not evolved, and a unit of machinability is not available. It should be noted that any statement regarding machinability may only apply under the particular set of circumstances existing when the observation was made. For example, under a given set of conditions a better surface finish may be obtained with material A than material B; however, under another set of conditions, say with a different tool material, the situation may be reversed. To complicate the situation further, if a certain group of materials is placed in order of machinability on a tool-wear basis, they may be placed in a different order if the surface finish or power-consumption criterion were to be applied. These objectives are not necessarily compatible hence, there is no single conclusive method of determining the machinabilities of work-piece materials.

As can be seen, machinability is a very complex subject. It has no universal unit and there is no single criterion for determining how 'machinable' a material is. In determining machinability of materials, it is vital that selected machinability criterion and all the used parameters must be stated clearly.

Machinability of a metal is affected from both cutting conditions i.e cutting speed, feed, depth of cut and also from the workpiece itself. In the case of steels, metallurgical considerations like hardness and microstructure greatly affects the machinability of steels and these effects are needed to be investigated thoroughly.

In determining machinability, several criterions are used. It is determined from life of the cutting tool i.e, how long a cutting tool perform its functions properly under definite conditions, or from the cutting speed at which metal is machined satisfactorily for a definite period, generally selected as 60 min. Other criterion for machinability is the power requirement for succeeding definite cutting operation

under specified conditions. In order to calculate the power requirement, forces produced during cutting are measured with special devices called dynamometers. All these methods are used in determination of the machinability properties of metals however, mostly used criterion is the tool life thus it gives very accurate results if performed under carefully planned conditions. The major disadvantage of this method is that it is a time and money consuming approach. In order to decrease these disadvantages, accelerated tests are also used but when these tests are applied, wear mechanism changes due to very high cutting speeds and reliability of the test results somewhat decreases.

1.2 Material Characterization by Non-Destructive Testing Methods

Hull [2] states that, since both individual components and complete engineering assemblies are subjected to various forces or loads, series of inspection and maintenance is necessary in order to eliminate malfunction or complete breakdown of these. A great number of instruments and techniques has been evolved over the years and new methods are still being developed to assist in the process of assessing the integrity and reliability of components and assemblies. Standard tests are applied to both components and assemblies on previously prepared test specimens. With these tests, important features of materials can be investigated including mechanical properties like tensile, compressive, shear and impact properties or other, but such tests are of a destructive nature. In order to perform these tests, specimens must be prepared from the component or assembly which means integrity of the system is no longer maintained. In addition, with these destructive tests, the material properties, not necessarily give a clear guide to the performance characteristics of a complex-shaped component which forms part of some larger engineering assembly.

Non-destructive testing (NDT) and evaluation methods are widely used in industry for various applications including quality check of the product, or maintenance in service. NDT can be defined as a test method for material inspection without altering or impairing its properties. It is very important that a non-destructively

tested product can perform its function completely after inspection thus, material is not damaged with these tests.

Non-destructive tests, especially ultrasonic testing can be used in determining the mechanical or other properties of materials. Since mechanical properties of materials strongly related to the microstructure, by observing microstructural changes with NDT methods, mechanical property changes of materials can be estimated. The use of NDT methods in these areas has been increasing due to their advantages over conventional destructive tests.

1.3 Aim of the Study

Machinability of a metal is affected from both cutting conditions and the metallurgical condition of the metal itself. This subject is attractive to scientists, and therefore many studies have been performed. Since it is known that microstructure, hardness and other metallurgical properties affects machinability, a further investigation need to be performed whether there is any correlation between other material property changes due to these effects. It is a known fact that, as a result of changes in the microstructure or hardness values, ultrasonic wave velocity also changes.

Investigation of the effect of the microstructural and hardness value changes on machinability properties of medium carbon steels is the major aim of this thesis. Correlation of these properties with the ultrasonic wave velocity measurements is also investigated.

In this thesis, effect of two different spheroidizing treatments and annealing heat treatment on machinability characteristics of two medium carbon steel types were analyzed, namely SAE/AISI 1040 and SAE/AISI 1050. Four sample groups have been prepared, one for the as-produced condition, two groups for spheroidizing treatment with different parameters and the last one for annealing treatment. After

the heat treatment operations were finished, hardness and ultrasonic wave velocities were measured, and metallographic investigation was performed. All these data were analysed in order to investigate possible correlations of these with machinability characteristics. For determining machinability properties of these workpieces, turning operation was applied on a standart engine lathe and tool wear at the tool flank change with respect to time is analyzed in order to reach the information necessary for the determination of the tool life.

On performing tool life tests, tool geometry, tool wear measurement and other test conditions were performed according to ISO 3685:1993E tool life testing with single-point turning tools standard. Cutting velocities were selected according to the capacity of the used engine lathe. Tool wear measurements were performed with tool maker's microscope.

CHAPTER II

HISTORICAL BACKGROUND

In 1969, Papadakis [3] amassed a comprehensive set of data on the attenuation and velocity of both longitudinal and transverse waves in hardened and tempered specimens of well known type of steel as functions of austenitizing temperature and ultrasonic frequency. He found that the attenuation is minimum in the fully hardened, fine grained specimen, and higher in the specimens austenitized at higher temperatures where austenitic grain growth is expected. It has also been observed that the ultrasonic velocity decreases with increasing austenitizing temperature.

In 1984, Papadakis [4] stated that physical acoustics could be used to investigate and inspect the microstructure of iron alloys in ways of interest and concern to both the academic and industrial communities. Results of his study showed that ultrasonic attenuation could make major contributions to the understanding and monitoring the microstructure. Also, he stated that ultrasonic velocity for monitoring the quality of ductile iron is the largest single application of physical acoustics to microstructure. He proposed, in general, physical acoustics could be used to monitor the various mechanisms that scatter and absorb elastic waves, and that cause variations in the elastic moduli of materials. Some of these mechanisms depend on frequency, so the proper frequency range of operation should be chosen. In particular, the monitoring of ductile iron quality is not dependent on frequency except in that frequencies above about 10-15 MHz do not penetrate the material adequately.

Murav'ev [5] investigated the influence of hardening, tempering, and annealing on the velocity of ultrasonic vibrations of 20, 250 mm x 30 mm x 10 mm steel

specimens in 38 KhA. The velocity of the ultrasonic wave was measured by the resonant method and by the method of auto circulation of pulses. The hardness was measured on a Brinell tester and the quantity of residual austenite and the intrinsic broadening were measured in parallel. The structure of the steel was determined by metallographic and electron microscopic methods after various forms and cycles of heat treatment. It has been reported that the velocity of propagation of ultrasonic surface waves in steel drops sharply after hardening in comparison with the original condition and increases with an increase in tempering time and temperature. He concluded that among other structural factors the phase composition of the alloy and the distortion of its crystalline lattice have the strongest influence on the velocity of propagation of an ultrasonic wave.

Prasad and Kumar [6] have correlated ultrasonic velocity and ultrasonic attenuation with the heat-treatment conditions of steel castings (i.e., cast, annealed, normalized, hardened and tempered conditions) in 1991. Steel samples of size 52 mm thickness and 52 mm diameter, melted in a direct arc-furnace were cast. Samples were annealed at 850°C, normalized at 850°C, and hardening was done at 820°C. Tempering temperatures were 200°C, 400°C and 600°C. For the purposes of velocity and attenuation measurement, a normal probe of 2.5 MHz, and of diameter 20 mm was used. Results showed that the longitudinal wave velocity is lower in the as cast condition compared with annealed or normalized samples. Also, the ultrasonic velocity is lower in a casting, which has been hardened, as compared to the annealed or normalized condition, but it is higher in the hardened and tempered condition. Also, the velocity increases with increasing tempering temperature. They concluded that, attenuation is highest in the as cast condition.

Later, Prasad and Kumar [7] have made an attempt to determine the influence of the deformation and the thermal treatment given to steel forging on the ultrasonic velocity and its attenuation. All parameters used in this study like samples, sample dimensions, heat treatment etc., were the same as the previous study explained above [27]. They observed that both the amount of deformation and the type of thermal treatment given to a forging influence the longitudinal wave velocity and

attenuation. With increasing degree of deformation, the ultrasonic velocity decreased, the velocity being found to be maximum for the normalized condition and the minimum for the hardened condition, in annealed samples the velocity lying between the two former values. Attenuation has been found to decrease with the degree of deformation and has been found to be minimum for the normalized case and maximum for the simply forged case.

In 1994, Vasudevan et.al. [8] characterized isothermal annealing of 20% cold worked Ti-modified 15Cr-15Ni-2.2Mo austenitic stainless steel (alloy D-9) by ultrasonic velocity measurements using a 2 MHz TR transducer. Furthermore, variation in ultrasonic velocity with ageing time was compared with that of hardness measurements. Alloy D-9 rods of 11 mm in diameter in the solution-annealed condition were deformed in tension to impart prior cold work of 20%. Ageing of samples cut from the cold worked rods were done at two different temperatures of 1073 K and 1123 K from 0,25 hr. to 220 hr. Vickers hardness was measured with a load of 10 kg. before and after the ageing treatment. Optical microscopy was used to study the microstructural changes. Results showed that ultrasonic velocity increased with ageing time in the recovery stage, was followed by a rapid decrease in the recrystallization stage, and reached saturation in the final stage due to completion of recrystallization. Wide differences in measured ultrasonic velocity values in the cold worked, recovered and recrystallized state of this material indicated that the technique used in experiments could be used effectively for studying microstructural changes during annealing of a cold worked metal. They concluded that, compared to hardness testing, technique used was a better tool for distinguishing between the recovery and recrystallization regimes distinctly.

Palanichamy et al. [9] have used ultrasonic velocity measurements to estimate average grain size in AISI type 316 stainless steel. The specimens used were heat treated at different temperatures varying from 1100°C to 1350°C for different time durations (15 min. to 120 min.) in order to obtain different grain sizes. All the specimens were given common heat treatment at 1050°C for 30 minutes followed

by water quenching to obtain uniform structure with same substructural features except variations in grain size. Metallographic examination was carried out to reveal the grain structure in different specimens. Ultrasonic velocity measurements were carried out using both longitudinal and shear wave normal probes with 2 MHz central frequency. They found a good correlation between the ultrasonic velocity measurements and metallographic measurements in grain size estimation. The maximum inaccuracy experienced in the estimation of average grain size using ultrasonic velocity measurements was 20%. The inaccuracy in grain size measurement was lower than that had been obtained by conventional attenuation measurement. The percentage change in velocity obtained for the grain size range that had been considered, i.e 60 to 170 μm , was smaller in the case of longitudinal waves (0,50%) as compared to shear waves (1,23%). Therefore, it had been concluded that shear waves would be more sensitive for grain size measurement. Also it was suggested that velocity measurements would give more accurate grain size measurements as compared to conventional attenuation measurements.

In 2000, Bouda, Boudai and Alem [10], measured ultrasonic velocity and attenuation by both longitudinal and transverse wave at the half cylindrical shape jominy specimens of steel. A correlation between ultrasonic measurements and steel hardness was investigated. Both immersion and contact coupling techniques was used. The longitudinal and transverse velocity and attenuation measurements showed the same appearance as hardness curves. A variation of attenuation of longitudinal and transverse waves have been observed and concluded that the reason of this variation is the structure homogeneity, included by carbon phase elements distributed differently inside the sample. In higher hardness zone, wave atenuation is most important due to the heterogeneity, where greatest wave diffusion is noted.

Bouda et al. [11] has developed an expeimental technique to measure velocities and attenuation of ultrasonic waves through the steel with a variable thickness. Steel samples were thermally processed to have gradient hardness lengthwise so as to characterise material hardness. An immersion technique was used for velocity and

attenuation measurements for both longitudinal and transverse waves. These measurements taken in immersion were done at oblique and normal incidence angles using a focussed probe. According to the results of measurements, it was possible to obtain the material hardness from its longitudinal or transverse velocity waves. This study showed that, it was possible and easy to obtain the material qualitative hardness from only one of these parameters: the longitudinal or transverse velocity wave, or its longitudinal or transverse attenuation.

Then, Vasudevan et. al. [12] characterized the microstructural changes of 20% cold worked annealed samples of alloy D9 by using longitudinal and shear wave velocities using 4 MHz probes. In this study, 6 and 8 mm of parallel-faced samples have been treated at 1073 K for different durations in the range of 0,5-1000 hours. Results showed that the variation in shear wave velocity with annealing time exhibited a three-stage behavior. It exhibits a slight increase in the recovery region up to 10 h followed by a sharp increase in the recrystallization region and reaches saturation after 500 h of annealing on completion of recrystallization . The trend exhibited by the shear wave velocity measurements during recrystallization is just opposite to that longitudinal wave. Shear wave velocities are found to be more sensitive than longitudinal wave velocity measurements in characterizing the annealing behaviour of cold worked austenitic stainless steel. Increase in sound velocities has been explained by the decrease in dislocation density during annealing.

In 2001, Lim and Lau [13] have investigated the effects of work material on tool wear rates using the wear map approach, through comparisons of the flank wear characteristics of TiC-coated cemented carbide tools during dry turning of two widely-used steel grades: a plain medium carbon steel (AISI 1045 equivalent) and a low-alloy medium carbon steel (AISI 4340 equivalent). The maps have demonstrated that tool wear rates vary with cutting speeds and feed rates used. They have also shown that there is a range of cutting conditions, called the safety zone, within which tool wear rates are the lowest. Wear maps constructed for the machining of AISI 1045 and 4340 steels show that flank wear is generally more

severe when machining the AISI 4340 grade, especially at high cutting speeds and feed rates. Nevertheless, the contour and location of the safety zone on the wear maps for both grades of steels correspond to that revealed in previous work on general steel grades. During their studies, the depth of cut was kept constant, no cutting fluid was used, and various combinations of cutting speed and feed rate were chosen for the tests with the aim of providing additional tool wear data for conditions that are not reported in the literature to ensure the proper construction of the wear maps later.

In 2003, Ozcatalbas and Ercan [14] have performed studies on investigation of the effects of microstructure and mechanical properties on the machinability of hot rolled SAE 1050 steel that was annealed and normalised before machining. The machinability has been characterised by measuring the tool life, chip root morphology, cutting forces, surface finish, and tool/chip interface temperature. The optimum machinability especially from the stand point of tool life, has been determined for hot rolled steel which had minimum impact energy and minimum ductility. By annealing this material, a coarse pearlitic microstructure and a microstructure having 10% spherical cementite was obtained with an increasing ferrite + pearlite banding. This led to an increase in ductility and impact energy, but the decrease in hardness shortened the tool life and worsened the machinability. With normalising heat treatment, on the other hand, the banding disappeared, hardness, ductility and impact energy increased; but the tool life shortened more and more. The maximum built-up edge (BUE) thickness occurred at lower cutting speeds in machining annealed specimens. The minimum surface roughness was observed on the hot rolled specimen at final cutting speeds. The heat treatment operations applied did not bring about a considerable difference in cutting forces. So, in their studies a significant correlation between the machinability and the hardness of specimens could not be determined.

Chou [15] hard turned different types of M50 steel (63 HRC) by using cubic boron nitride (CBN) tools to experimentally investigate microstructural effects on both continuous and intermittent cutting. In continuous cutting, powder metallurgy (PM)

M50 results in substantially lower tool wear and wear rate than conventional M50, presumably due to refined carbides that may delay delamination wear. In intermittent cutting, fine microstructures of PM steel also lead to reduced wear rate, however, not as drastically as in continuous cutting. In intermittent cutting, the bulk impact loading may be dominant in tool wear and attrition wear affected by carbide sizes becomes less significant. Nevertheless, fine carbides in PM steel seem to alleviate delamination wear on tool flank, which limits tool life at lower speed in intermittent cutting of conventional M50. Furthermore, low CBN content tools consistently outperform high CBN content tools in PM M50 intermittent cutting, contradictory to the results in intermittent cutting of conventional counterparts.

In 2003, Tekiner and Yesilyurt [16] have studied on determination of the best suitable cutting conditions and cutting parameters during machining of AISI 304 stainless steels by taking into consideration process sound. For determination of the best cutting parameters in the stainless steels machining, the samples which were prepared, 200 mm in length and 30 mm in diameter, and were machined in a CNC turning centre. Each part of samples was machined through the 150 mm length and the depth of cut was 2.5 mm. Turning tests were performed with three different feed rates (0.2, 0.25, 0.3 mm/rev) at each cutting speed, 120, 135, 150, 165, 180 m/min. During experiments, process sounds were recorded by a computer incorporating a microphone. The best cutting speed and feed rate were determined according to flank wear, built up edge, chip form, surface roughness of the machined samples and machine tool power consumption. The ideal cutting parameters and cutting process sounds obtained were compared. In this way, the best cutting parameters could be determined depending on the sound. Finally, cutting speed of 165 m/min and feed rate of 0.25 mm/rev gave the best results and the analyses of the process sound confirmed these values.

Korkut, Kasap and Şeker [17] have made studies on determination of the optimum cutting speed when turning an AISI 304 austenitic stainless steel using cemented carbide cutting tools. The influence of cutting speed on tool wear and surface roughness was investigated. A decrease in tool wear was observed with increasing

the cutting speed up to 180 m/min. Surface roughness (R_a) was also decreased with increasing the cutting speed. Correlation was made between the tool wear/surface roughness and the chips obtained at the three cutting speeds of 120, 150 and 180 m/min. Feed rate and depth of cut were kept fixed, 0.24 mm/rev and 2.5 mm, respectively. The cutting speeds were chosen by taking into consideration the cutting tool manufacturer's recommendations and industrially used values for this material. Tool flank wear and tool-chip contact length on the tool rake face were measured using a Stereo Zoom Microscope and surface roughness was measured using a portable Mahr Perthometer M2 instrument. The criterion for the tool life was 0.3 mm flank wear (V_B). They concluded that, tool flank wear decreased with increasing the cutting speed up to 180 m/min. The poor performance of the tool could well be explained by the thermal softening of the tool due to the higher influence of the heat on the cutting tool and less efficient heat dissipation at the lower cutting speeds.

Sikdar and Chen [18] have studied on the relationship between flank wear area and cutting forces for turning operations. A set of experiments were performed on a CNC lathe without coolant. The CNMG120412N-UJ tool insert was used to cut low alloy steel (AISI 4340). Flank wear surface area was measured by surface texture instrument using a software package. Cutting forces were measured by a Kistler piezo-electric dynamometer. The experimental results show that there is an increase in the three directional components of the cutting force with increase in flank wear area. Among the three cutting forces measured, the tangential force was the largest while the radial force is the smallest. However, when the tool insert begins to fail, all the three cutting forces increase sharply, especially so for the axial and radial cutting forces. The radial force was also found to be slightly larger than the axial force when tool begins to fail.

Paro, Hanninen, and Kauppinen [19] have worked on active wear and failure mechanisms of TiN-coated cemented carbide tools when machining X5 CrMnN 18 18 austenitic stainless steel. By nitrogen alloying austenite was stabilised and the strength of austenitic stainless steel was increased and work hardening was

promoted. High strength and work hardening rate cause difficulties from the machining point of view. In their study turning tests carried out by using a test lathe and a cutting force measuring device were presented. Chips were analysed by scanning electron microscopy. The machinability of X5 CrMnN 18 18 austenitic stainless steels was examined based on tool life and cutting speed presented by v-T diagrams. The effect of cutting speed and nitrogen content was also analysed by cutting force measurements. Based on the cutting tests, cutting speeds of 40–200 m/min, feed rate of 0.15–0.25 mm and depth of cut of 1.6 mm for X5 CrMnN 18 18 stainless steels could be applied from machinability point of view. Higher nitrogen content decreases cutting force and decreases machinability. Tool wear criterion, VB-value of 0.3 mm, was reached after turning time of 10 min, when 60, 65 and 70 m/min and 0.24 mm/r feed rates were utilised.

Benga and Abrao [20] have studied on machinability of hardened 100Cr6 bearing steel (62–64 HRC) when continuous dry turning using mixed alumina, whisker reinforced alumina and polycrystalline cubic boron nitride (PCBN) inserts. A full factorial experimental design was employed and the cutting range tested was as follows: cutting speed varying from 70 to 210 m/min and feed rate from 0.08 to 0.28 mm/rev. Tool life and surface finish were evaluated. As far as tool life is concerned, best results were obtained with the PCBN compact, followed by the mixed alumina tool at low feed rates and by the whisker reinforced alumina when feed rate was increased. Comparable surface roughness values were produced, with R_a values as low as 0.25 μm .

CHAPTER III

CONCEPT OF MACHINABILITY

3.1 Measures of Machinability

Historically, machinability of a material can be assessed with one of the following criteria: cutting speed, power consumption, surface finish and tool life.

According to Childs, Meakawa, Obikawa and Yamane [21], in the **cutting speed method**, machinability is estimated by measuring the maximum speed at which a standard tool under standard conditions can continue to provide satisfactory performance for a specified period. Generally, the period is selected as 60 minutes. In order to compare and rank materials, a common material is taken as a reference or standard. The machinability of any other material may be compared to the standard, usually B1112 steel, by determining the V_{60} (or V_{90}) and taking the ratio (V_{60} material/ V_{60} standard) and expressing it as a percentage. This ratio is called relative machinability. Clearly, a material with a high cutting speed for a 60-minute tool life will be considered to have a high machinability, which is desirable. Handbooks and manuals contain data on relative machinability for the convenience of users. This allows various materials to be compared; the higher the relative machinability, the easier is the material to machine from the point of view of tool wear and tool life. Thus, when assessed in this way machinability is essentially equivalent to tool life with particular reference to the effect of work material.

A tool-life equation with V_{60} representing machinability can be expressed as:

$$V_{60} = A_1 \frac{k}{l.(B.H.N)} \left(1 - \frac{A_r}{100}\right)^{1/2} \quad (3.1)$$

where,

V_{60} : Cutting speed for a 60-minute tool life (m/min),

A_1 : Constant,

l : Characteristic length (m),

B.H.N : Brinell hardness number of the work material,

A_r : Percent area reduction ratio of work material in tension

A_r can be expressed as:

$$A_r = \frac{\text{Initial Area} - \text{Final Area}}{\text{Initial Area}} \times 100 \quad (3.2)$$

Boulger [22] states that, in the **power consumption method**, machinability is estimated by measuring the power required to remove a unit volume of material under specified machining conditions. The forces acting on a tool during cutting, as measured on a dynamometer, can be used to estimate the power consumed in metal cutting. The power consumption is approximately equal to the product of the cutting velocity, V , and the component of cutting force parallel to the cutting direction, F_T . To calculate the unit power consumption, which reflects the power requirements for cutting a particular material, it is necessary to divide the power consumption by the metal removal rate, which is, for turning the product of the cutting velocity times the feed times the depth of cut. Unit power consumption increases with increasing hardness, which reflects the resistance of the material to the deformation required in machining operations.

The unit power consumption is given by:

$$P = \frac{F_T}{f \cdot d} \quad (3.3)$$

where,

- P : Power (in Megajoules),
- F_T : Cutting force (in Newtons),
- f : Feed (in mm),
- d : Depth of cut (in mm),

In the **surface finish method**, machinability is estimated by examining surface quality of the machined product. A smooth surface is a desired material property thus, low friction, closer tolerance and load carrying capacity is strongly related to the surface quality. Due to these reasons, surface roughness is an important design factor. In this method, surface is examined by some special instruments and variations in the surface finish is determined. When the surface finish becomes not satisfactory, tool life is thought to be over. This method gives qualitative results. Due to the need of very precise examination, it is not an easy method for estimating machinability.

Trent [23] states that, in normal workshop practice, it is necessary to regrind a cutting tool when the shape has been so altered that it can no longer cut efficiently, or is about to fail in this way. Here, the most important consideration is that tools to be used until they are worn to a condition just short of that at which extensive regrinding would be necessary, they should be run only to the point where regrinding is still economical of time and tool material. The amount of work done by the tool between regrinds is called the **life of the tool**, and this may be measured in a number of different units, depending on the character of the machining operation: in units of time, or number of components machined, or weight of the metal removed before the end of tool life.

Under actual cutting conditions, the cutting temperatures and stresses are very high, causing the tool to decrease in hardness and undergo plastic deformation. Tool life depends to a very great extent on the cutting velocity and in decreasing order to lesser extent in feed, depth of cut, and workpiece material. In roughing operations, the various tool angles, cutting speeds, and feed rates are usually chosen to give an economical tool life. Conditions giving a very short tool life will be uneconomical because tool-grinding and tool replacement costs will be high. On the other hand, the use of very low speeds and feeds to give long tool life will be uneconomical because of the low production rate [1].

Tool life and cutting speed can be related by the equation:

$$V \cdot T^n = C \quad (3.4)$$

where,

- V : Cutting speed (m/min)
- T : Tool life (min)
- C, n : Empirical constants

Equation 3.4 is known as Taylor equation after his studies for tool life determination for single-point turning. Constant C is known as Taylor constant. Value of n is related to the tool material and it is generally between 0,1 and 0,2 for high-speed steel tools. Cutting velocity is the major parameter in determining tool life and small changes in cutting speeds results in great changes in tool life.

A more sophisticated deterministic expression for relating tool life to cutting speed, feed and depth of cut has the form:

$$V^{1/n} \cdot T \cdot f^{m/n} \cdot d^{p/n} = C \quad (3.5)$$

where,

f : Feed (mm/rev),
d : Depth of cut (mm),
C, m, n, p: Empirical constants

In determining tool life, several criterions are used. In one type of criterion, tool life is determined from catastrophic failure of the tool. In another criterion, tool life is considered to be over when surface finish of the workpiece becomes unacceptable. In another type of criterion, when a definite form of wear on tool reaches a predetermined value, tool life ends. This approach has many advantages over catastrophic failure approach thus testing time and testing costs are lower and for these reasons it is the most commonly used tool-life criterion. Quantitative results are achieved from this method and these results can be used in equations in order to achieve the sort of ordering of information characteristic of engineering approach.

3.2 Tool Life and Tool Wear

3.2.1 Wear and Wear Mechanisms

The fundamental nature of the mechanism of wear can be very different under different conditions. In metal cutting, three main forms of wear are known to occur: adhesion, abrasion, and diffusion wear.

In adhesion wear, wear is caused by the fracture of welded asperity junctions between the two metals. In metal cutting, junctions between the chip and tool materials are formed as part of the friction mechanism; when these junctions are fractured, small fragments of tool material can be torn out and carried away on the underside of the chip or on the new workpiece surface.

The abrasion wear occurs when hard particles on the underside of the chip pass over the tool face and remove tool material by mechanical action. These hard particles

may be highly strain-hardened fragments of an unstable built up edge, fragments of the hard tool material removed by adhesion wear, or hard constituents in the work material.

Solid state diffusion occurs when atoms in a metallic crystal lattice move from a region of high atomic concentration to one of low concentration. This process is dependent on the existing temperature, and the rate of diffusion increases exponentially with increases in temperature. In metal cutting, where intimate contact between the work and the tool materials occurs and high temperatures exist, diffusion can occur where atoms move from the tool material to the work material. This process, which takes place within a very narrow reaction zone at the interface between the two materials and causes a weakening of the surface structure of the tool, is known as diffusion wear [1].

3.2.2 Forms of Wear in Metal Cutting

The progressive wear of a tool takes place in two distinct ways:

1. Crater wear forms on the tool region where chip flows over it.
2. Flank wear forms on the tool region where tool is in contact with the newly machined workpiece surface.

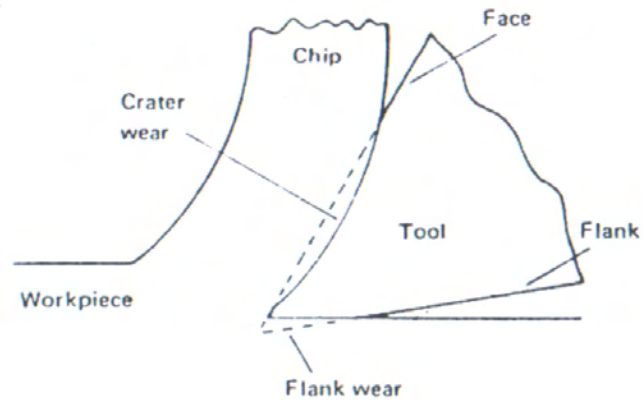


Figure 3.1: Regions of tool wear in metal cutting [1]

3.2.2.1 Crater Wear

The surface over which the chip passes, see Figure 3.1, is called the rake face of the tool. On rake face, wear takes the form of a cavity or crater. It has its origin not along the cutting edge but at some distance away from it and within the chip contact area.

According to Mills and Redford [24], because of the stress distribution on the tool face, the frictional stress in the region of sliding contact between the chip and the face is at a maximum at the start of the sliding contact region and is zero at the end. Thus abrasive wear takes place in this region with more wear taking place adjacent to the seizure region than adjacent to the point at which the chip loses contact with the face. This results in localised pitting of the tool face some distance up the face which is usually referred to as cratering and which normally has a section in the form of a circular arc.

As the wear progresses with time, the crater gets bigger and approaches the edges of the tool. Crater wear is usually associated with ductile materials which give rise to continuous chips with built-up edge. If crater wear is allowed to proceed too far, the cutting edge becomes weak as it thins out, and breaks down suddenly. In general crater wear develops faster than flank wear on ductile materials.

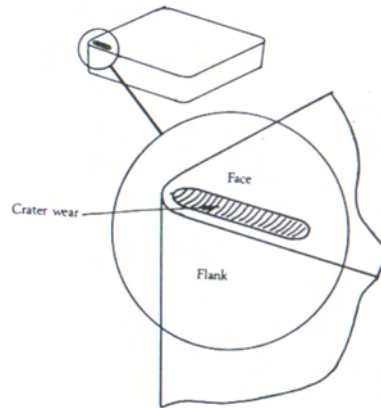


Figure 3.2: Crater wear on an indexable insert [24]

The crater formed on the tool face conforms to the shape of the chip underside and is restricted to the chip tool contact area, see Figure 3.2. In addition, the region adjacent to the cutting edge where sticking friction or a built-up edge occurs is subjected to relatively slight wear. Under high-temperature (in the order of 1000°C) metal cutting conditions, high-speed steel tools will wear very rapidly because of thermal softening of the tool material. With carbide - tool materials, although they retain their hardness at these high temperatures, solid state diffusion can cause rapid wear. In experimental work, the maximum depth of the crater is usually a measure of the amount of crater wear and can be determined by a surface measuring instrument. Under very high-speed cutting conditions, crater wear is often the factor which determines the life of the cutting tool: the cratering becomes so severe that the tool edge is weakened and eventually fractures. However, when tools are used under economical conditions, the wear of the tool on its flank, known as flank wear, is usually the controlling factor [1].

3.2.2.2 Flank Wear

Clearance face of the cutting tool along which the major cutting edge is located, see Figure 3.1, is called the flank face. At chip separation point, it is the portion of the tool that is in contact with the work material and that resists the feeding forces.

Because of clearance, initial contact is made along the cutting edge. Flank wear begins at the cutting edge and develops into a wider flat of increasing contact area called a wear land. Wear on the flank of a cutting tool is caused by friction between the newly machined workpiece surface and the contact area on the tool flank. Because of the rigidity of the workpiece, the worn area, referred to as the flank wear land must be parallel to the resultant cutting direction.

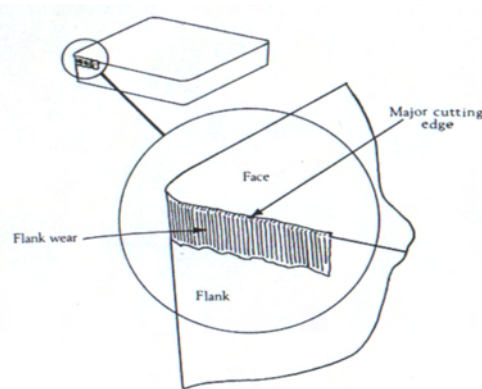


Figure 3.3: Flank wear on an indexable insert [24]

Flank wear occurs under almost all conditions of cutting, but metallographic evidence shows that more than one wear process is involved, so that simple laws relating the rate of wear to variables such as speed, feed, tool geometry, etc. can be expected only under conditions where the wear process remains substantially unaltered. Cutting tools are generally used most efficiently when the only form of wear is an even land on the tool flank, but factors other than flank wear influence the life of tools in practice. The width of the wear land is usually taken as a measure of the amount of wear and can be readily determined by means of a toolmaker's microscope. Flank wear often takes the form of an even band of wear, the depth of which can be measured with reasonable accuracy. When the worn tool surfaces are examined under the microscope they are often found to be wholly or partly covered by a layer derived from the work material. This may be relatively thick, in the form known as a built-up edge, or a thin smear a few microns or a

fraction of a micron thick. The flank surface of a tool tip is lapped optically flat and the tip is then clamped in a tool holder and used for cutting under controlled conditions. After cutting, any deformation of the tool tip can be observed and measured by placing the flank surface of the tip on a flat glass plate and examining it under monochromatic light [23].

For practical cutting conditions, crater wear is a less severe than flank wear and consequently flank wear is a more common tool failure criterion. At the end of the major flank wear land where the tool is in contact with the uncut workpiece surface it is common for the flank wear to be more pronounced than along the rest of the wear land. This is because of localised effects such as a hardened layer on the uncut surface caused by work hardening introduced by a previous cut, an oxide scale, and localised high temperatures resulting from the edge effect. This localised wear is usually referred to as notch wear and occasionally is very severe. Although the presence of the notch will not significantly affect the cutting properties of the tool, the notch is often relatively deep and if cutting were to continue there would be a good chance that the tool would fracture [23].

3.2.3 Tool Wear Measurement

A tool life criterion is defined as a predetermined threshold value of a tool-wear measure or the occurrence of a phenomenon. In practical machining operations the wear of the face and flank of the cutting tool is not uniform along the active cutting edge; therefore it is necessary to specify the locations and degree of the wear when deciding on the amount of wear allowable before regrinding the tool.

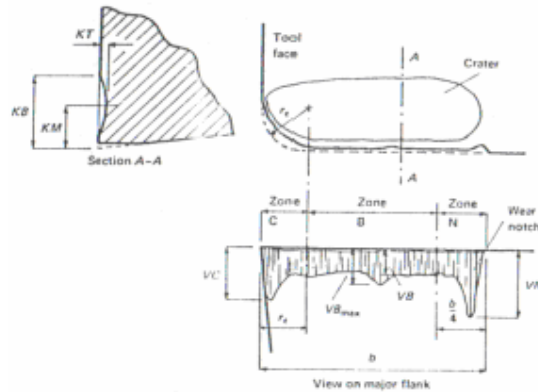


Figure 3.4: Some features of single-point tool wear in turning operations [1]

Figure 3.4 shows a typical worn single-point tool. As shown in the figure, the amount of cratering varies along the active cutting edge, and the crater depth KT is measured at the deepest point of the crater (section AA). It can be seen that flank wear is usually greatest at the extremities of the active cutting edge. Conditions at the tool corner tend to be more severe than those in the central part of the active cutting edge because of the complicated flow of chip material in that region. The width of the flank wear land at the tool corner (zone C) is designated VC . At the opposite end of the active cutting edge (zone N) a groove or wear notch often forms because in this region, the work material tends to be work-hardened from the previous processing operation. The width of the wear land at the wear notch is designated VN . In central portion of the active cutting edge (zone B), the wear land is fairly uniform. However, to allow for variations that may occur, the average wear-land width in this region is designated VB and the maximum wear-land width is designated VB_{max} [1].

In the ISO 3685:1993 Tool life testing with single-point turning tools standard [25], tool life criterion for H.S.S tools in terms of flank wear is stated as:

- a) $VB_{max} = 0.6$ mm (max. width of flank wear land) if flank not irregularly worn, scratched, chipped or badly grooved in zone B

- b) Average width of flank wear land $VB_B = 0.3$ mm if flank is regularly worn in zone B
- c) Catastrophic failure

3.2.4 Tool Wear and Time Relation

Cutting time is an important factor in tool life testing. Performing test until the catastrophic failure of the tool has some disadvantages. First disadvantage is that it is time and material consuming in a great extent. By taking into account the importance of time and economics, it is clear that this approach is not feasible. Another disadvantage is that tool can be only examined at the end of the tool life and the preliminary stages of the tool wear cannot be examined. For these reasons, it is logical that selecting one of the predetermined wear criterions mentioned in the section 3.2.2.

Crater wear, normally measured in terms of the depth of the crater, increases progressively with time until a point is reached when the crater weakens the tool sufficiently for the forces acting on the tool to fracture it. Thus the criterion for tool failure due to crater wear is based on a crater depth of a constant amount plus a further amount which is proportional to the feed. Catastrophic failure of high-speed steel tools is merely an extension of the flank wear criterion for carbides and follows the same type of relationship with time. All other forms of wear which result in rapid deterioration of the tool are often difficult to relate to time in a meaningful manner since the tool can fail when there is little or no wear and this can often be due to a transient condition in that is basically a steady-state operation.

For progressive flank wear the relationship between tool wear and time follows a fixed pattern. Initially, with a new tool, the wear rate is high and is referred to as primary wear. The time for which this wear rate acts is dependent on the cutting conditions but, typically, for a given workpiece material, the amount of primary

wear is approximately constant but the time to produce it decreases as the cutting speed is increased. This wear stage is followed by the secondary wear stage where the rate of increase of flank wear is sensibly constant but considerably less than the rate of primary wear in the practical cutting speed range. At the end of the secondary wear stage, when the flank wear is usually considerable and far greater than that recommended as the for tool failure, the conditions are such that a second rapid wear rate phase commences (tertiary wear) and this, if continued, rapidly leads to tool failure [24].

The three stages of wear are illustrated in Figure 3.5:

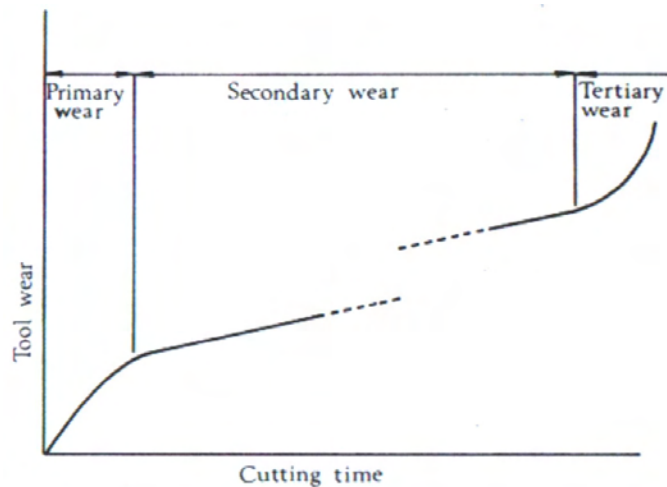


Figure 3.5: Typical relationship between flank wear and cutting time [24]

3.2.5 Determination of Tool Life

If life of the cutting tool is determined for different cutting velocities and these data taken into a graph, a pattern similar to the Figure 3.6 can be achieved thus it represents the typical relationship between tool life and cutting velocity. It can be seen that as cutting velocity increases, tool life reduces dramatically.

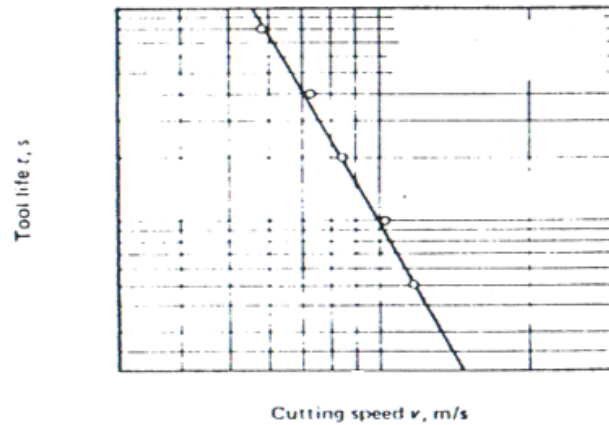


Figure 3.6: Typical Relationship Between Tool Life and Cutting Speed [1]

F.W. TAYLOR [26] has performed tests on metal removing to determine the correlation between cutting velocity and tool life. He established the well known equation, which is mentioned in the section 3.1.4, $V \cdot T^n = C$ as a result of these studies where, V is cutting speed (m/min), T is tool life (min), C is Taylor's constant and n is a constant which can be found from the slope of the tool life vs. cutting velocity graph.

Significant changes in the tool geometry, depth of cut, and feed will change the value of the constant 'C', and may cause a slight change in the exponent 'n'. In general 'n' is a more function of the tool material, than other parameters. Tool life is most sensitive to changes in cutting speed, less sensitive to changes in feed, and least sensitive to changes in depth of cut.

3.3 Turning Operation

This basic work is also the one most commonly employed in experimental work on metal cutting. The work material is held in the chuck of a lathe and rotated. The tool is held rigidly in a tool post and moved at a constant rate along the axis of the bar,

cutting away a layer of metal to form a cylinder or a surface of more complex profile.

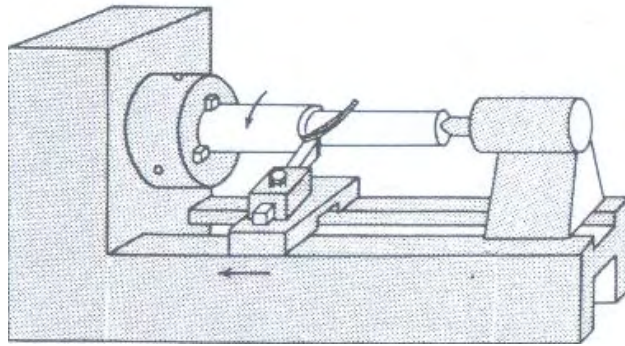


Figure 3.7: Illustration of the turning operation [27]

According to Trent [27], the cutting speed (V) is the rate at which the uncut surface of the work passes the cutting edge of the tool—usually expressed in units of m/min or ft/min. The feed (f) is the distance moved by the tool in an axial direction at each revolution of the work. The depth of cut is the thickness of metal removed from the bar, measured in a radial direction. The cutting speed and the feed are the two most important parameters which can be adjusted by the operator to achieve optimum cutting conditions. The rotational speed (rpm) of the spindle is usually constant during a single operation so that, when cutting a complex form the cutting speed varies with the diameter being cut any instant. At the nose of the tool the speed is always lower than that at the outer surface of the bar, but the difference is usually small and the cutting speed is considered as constant along the tool edge in turning.

3.4 Chip Formation

In the formation of chip, early ideas proposed theories based on a ‘splitting’ of the workpiece material ahead of the cutting tool but this explanation was soon discarded in favour of the shear plane theory which suggests that the chip is formed

during machining by fracture along successive shear planes which are inclined to the direction of cutting. Chips can be either continuous or discontinuous [24].

Enahoro and Welsh [28] states that, in the discontinuous chip formation, segments are formed by rupture which occurs intermittently and is observed to take place ahead of the tool, leaving a rough and irregular surface. Almost without exception, a discontinuous chip is formed in all machining operations involving brittle materials such as brass or cast iron. Under certain conditions this also occurs with ductile materials.

During the formation of a chip the material undergoes severe strain, and, if the work material is brittle, fracture will occur in the primary deformation zone when the chip is only partly formed. Under these conditions the chip is segmented [1].

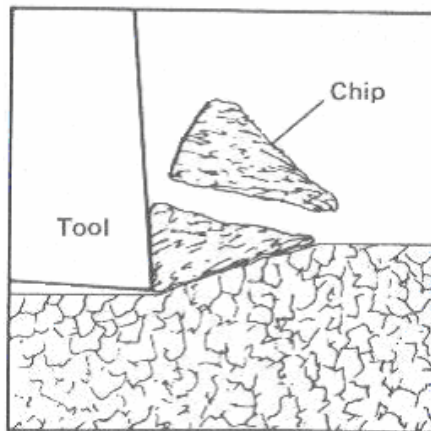


Figure 3.8: Discontinuous chip [1]

Continuous chip is common when cutting a ductile material such as mild steel under favorable conditions such as good lubrication between chip and tool. It can be seen that cutting under these conditions is a steady-state process. For this reason most of the research conducted into metal cutting has dealt with continuous chip production. Basically this operation is one of shearing the work material to form the chip and

the sliding of the chip along the face of the cutting tool. The resulting machined surface is smooth [1].

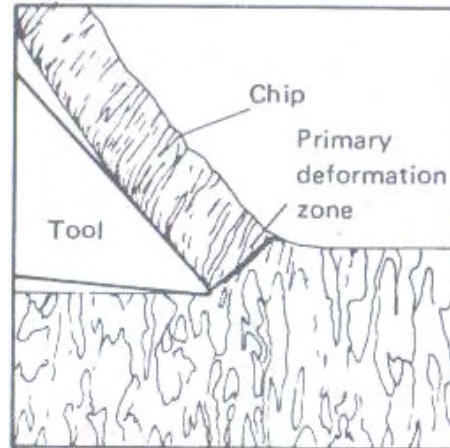


Figure 3.9: Continous chip [1]

Under certain conditions, when producing a continuous chip, a zone of highly deformed material adheres to the tool near the cutting edge. This has been named the built-up edge and is usually found welded to the tool after a machining operation. This type of chip is formed as a result of the high value of tool/chip interface action, which is a deciding factor in determining the type of chip formed. The built-up edge is work-hardened material and is one of the causes of bad finishes in machined surfaces; the built-up edge is not stable, but periodically builds up and breaks down; some parts of it are carried away in the chip while other parts are left embedded in the surface, thus marring it. This type of chip is obtained when machining ductile materials at low speeds [28].

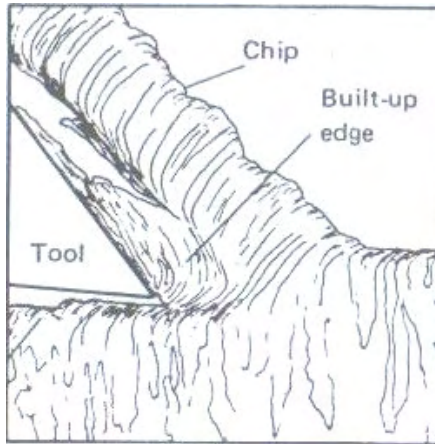


Figure 3.10: Continuous chip with built-up edge [1]

3.5 Cutting Tools

Edwards [29] states that, cutting tools employ a wedging action. All the power used in cutting metal is ultimately expended in heat. A tool that has been used on heavy cuts has a small ridge of metal directly over the cutting edge. This bit of metal is much harder than the metal being cut, and is almost welded to the edge of the tool, indicating that an immense amount of heat and pressure was developed. In high-speed production work, coolants help absorb the heat from the cutting edge of the tool. A steady stream of cutting compound should be directed at the point of the cutting tool, so that it spreads and covers both the cutting tool and the work.

There are several different materials used to make cutting tools or cutter bits. In order to machine metal accurately and efficiently, it is necessary to have the proper lathe tool ground for the particular kind of metal being machined, with a keen, well supported cutting edge. Some of the materials used to make cutting tools are:

- Carbon steel cutting tools are less expensive, and can be used on some types of metal successfully.

- High-speed steel cutting tools are the most popular type of lathe tools. They will withstand higher cutting speeds than carbon steel cutter bits.
- Stellite cutting tools will withstand higher cutting speeds than high-speed ones. Stellite is a nonmagnetic alloy which is harder than common high-speed steel.
- Carbide cutting tools are made of carbide for manufacturing operations where maximum cutting speeds are desired. Mostly used ones are tungsten carbide, tantalum carbide and titanium carbide [29].

The cutting end of the cutting tool is adapted to its cutting requirements by grinding its sides and edges at various angles. Since the cutting tool is more or less tilted in the toolholder, the angles are classed as either tool angles or working angles.

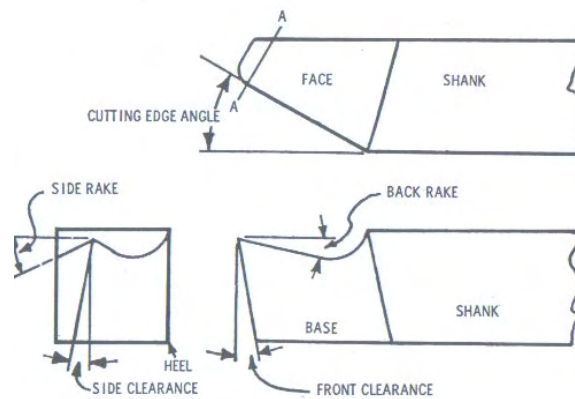


Figure 3.11: Illustration of cutting tool rake and clearance angles [29]

- Top back rake is the inclination of the face of a tool to or from the base. If it inclines away from the base, the rake angle is positive. If it inclines away from the base, the rake angle is negative. The cutting angle should be as large as possible for maximum strength at the edge and to carry heat away

from the cutting edge. On the other hand, the larger the cutting angle, the more power is required to force it into the work.

- Side rake angle is the angle between the face of a tool and a line parallel to the base. The cutting tool will not cut without side rake, and this angle relieves excessive strain on the feed mechanism also varies with the material being machined.
- Front clearance angle is between the flank and a line from the cutting edge perpendicular to the plane of the base. Front clearance depends somewhat on the diameter of the work to be turned.
- Side clearance is the angle between the side of a tool and a line from the face edge perpendicular to the plane of the base. In turning, the clearance angle allows the part of the tool bit directly under the cutting edge to clear the work while taking a chip [29].
- Side relief angle is between the portion of the side flank immediately below the side-cutting edge and a line drawn through this cutting edge perpendicular to the base. It is usually measured in a plane at right angles to the side flank and hence is normal side relief.
- Oxley [30] states that, end relief angle is between the portion of the end flank immediately below the end-cutting edge and a line drawn through that cutting edge perpendicular to the base. It is usually measured in a plane at right angles to the end flank and hence is normal end relief.

CHAPTER IV

FACTORS AFFECTING MACHINABILITY OF STEELS

4.1 Chemical Composition

According to Lane, Stam, and Wolfe [31], the way in which the chemical composition of a steel affects its machinability is directly associated with the way in which this composition affects the ultimate hardness of the steel. From this it may be appreciated that, as carbon is the major element which increases the hardness, then an increase in the content of this element causes profound changes in machinability. At room temperature iron dissolves carbon up to 0.025%. With the carbon content in this low range the structure is a homogenous α -solid solution which is soft and ductile. As the carbon content is increased above 0.025% the excess carbon forms iron carbide which cannot be held in solid solution by the iron at room temperature. The iron carbide then exists as a separate constituent generally in the form of pearlite, which strengthens and hardens the iron matrix and reduces its ductility. The improvement in machinability which comes from the loss in ductility more than compensates for this decrease as the result of increased hardness. The net result is, therefore, an increase in machinability. However, once the carbon content of a steel exceeds 0.4% (200 HB) further increase reduces its machinability.

Other than carbon, there are other elements which affect the machinability of a steel. They do not affect the hardness values of steel like carbon but other factors are present. There is a steel type called 'free machining steels' and as can be understood from the name, their machinability values are very higher than the other steel types including plain carbon steels, low alloy steels or high alloy steels.

Generally free machining steels are produced by addition of Pb about 0.3%. Lead is present in the matrix as evenly distributed globules and they act as solid lubricant. This means, presence of lead reduces the friction between tool and the steel which results lower cutting temperatures and longer tool life.

On the other hand, additions of sulphur, selenium, and zirconium, together with controlled amounts of manganese, also forms well distributed sulphides and selenides in the matrix. They act as stress raisers in the chips-which results in their breaking down into small segments during the machining operation and so reducing the frictional load on the tool. By this, continuous chip and built-up edge formation is eliminated.

Table 4.1: Machinability Effect of Alloying Elements

Affecting Negatively	Ni, Co, Cr, V, C (<0.3%), C (>0.6%), Mo, Nb, W
Affecting Positively	Pb, S, P, C (0.3-0.6 %), Zr, Se

4.2 Hardness

Hardness of a steel is considered to be a good parameter relating with the machinability. Generally it is considered that as hardness increase machinability decreases but it is partly true. Steels with very high hardness levels have lower machinability but reverse case is not true. Very soft steels are also machined poorly because of the other factors, including their high ductility.

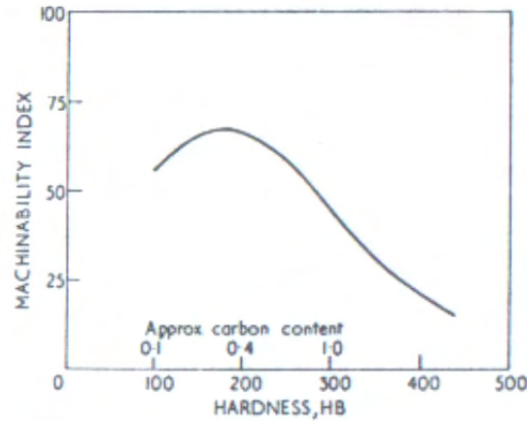


Figure 4.1: Effect of hardness on machinability [31]

When comparing various steels with hardnesses greater than 250 HB, the machinability varies almost inversely with the hardness, while steels softer than 250 HB do not always follow this rule owing to the interaction of other factors such as composition, microstructure and ductility. The most satisfactory hardness for general machining of steel is about 180 HB. Below this hardness steels usually have relatively high ductility resulting in a greater tendency to develop a built-up edge on the tool. With soft steels the low machinability results from the high ductility which permits considerable deformation of the metal during machining. A built-up edge generally occurs at the tip of the tool, and the chip formed is of the undesirable continuous type. Speeds must be limited to prevent burning the tool and a rough, undesirable finish is often produced when machining these softer grades of steel. A comparatively large number of machining problems have been encountered when machining steels at hardness below 160 HB. With hardnesses above 200 HB there is a gradual decrease in machinability with increase in hardness and under these conditions the importance and influence of other factors reduced, since microstructure, ductility and other characteristics are uniform, changing only gradually with change in hardness. The limit of hardness for machining is often considered to be about 350 HB, above which steels are sometimes classified as commercially unmachinable. This does not mean that steels of higher hardness cannot be machined, but that at higher hardness the speeds must be reduced to a

point at which machining costs become excessive. From this it may be appreciated that, as carbon is the major element which increases the hardness, then an increase in the content of this element causes profound changes in machinability, although other factors, such as microstructure, have certain limiting effects [31].

Formula has been developed for showing the relationship between hardness, ductility and cutting speed for a 60-min tool life is:

$$V_{60} = \frac{C}{B^{1.63}R^{1.01}} \quad (4.1)$$

where,

- V_{60} : Cutting speed for a 60 min tool life (m/min),
- C : Constant,
- B : Brinell hardness,
- R : Reduction in area %

Constant C varies with the form and size of the tool used, the steel from which the tools are made and their heat treatment, as well as the feed and depth of cut.

4.3 Microstructure

Carbon content has a dominant effect on the machinability of carbon steels, chiefly because it governs strength, hardness and ductility. Increasing the carbon content of steel increases the strength and unit power consumption for cutting. The microstructure of low-carbon steel may have large areas of ferrite interspersed with small areas of pearlite. Ferrite is soft, with high ductility and low strength, whereas pearlite, a combination of ferrite and iron carbide, has low ductility and high strength. Low carbon steels containing less than 0.15% carbon are low in strength in the annealed condition; they machine poorly because they are soft and gummy and adhere to the cutting tools. The machinability of these grades can best be improved

by work hardening to raise the strength level and lower the ductility. Steels in the 0.15 to 0.30% carbon range are usually machined satisfactorily in the as-rolled, as-forged, annealed or in the normalized condition with a predominantly pearlitic structure. The medium carbon grades, containing up to about 0.55% carbon, machine best if an annealing treatment that produces a mixture of lamellar pearlite and spherodite is utilized. If the structure is not partially spherodized, the strength and hardness may be too high for optimum machinability.

A greater amount of pearlite is present in high-carbon steels because of the higher carbon content. The greater the amount of pearlite (low ductility and high strength) present in the steel, the more difficult it becomes to machine the steel efficiently. For steels with carbon content higher than about 0.55%, a completely spherodized structure is preferred. It is therefore desirable to anneal these steels to alter their microstructures and, as a result, improve their machining qualities. Hardened and tempered structures are generally not desired for machining [4].

Table 4.2: Optimum microstructures for best machinability ratings [22]

Carbon %	Optimum Microstructure
0.06-0.20	As rolled (most economical)
0.20-0.30	Under 3 in. dia., normalized; 3 in. dia. and over, as rolled
0.30-0.40	Annealed to give coarse pearlite, minimum ferrite
0.40-0.60	Coarse lamellar pearlite to coarse spherodite
0.60-1.00	100 % spherodite, coarse to fine

A steel with a small austenitic grain size (less than 5 on ASTM scale) absorbs more power in machining than does one with a larger grain size, provided other things are equal. Fine grained steels (less than 5) produce a finish superior to coarse-grained steels on finish machining [31].

Banded structures and structures showing coarse and fine ferritic grains in adjacent positions are usually unsatisfactory as they result in inferior finishes and a short tool

life. Carbon steels nearly always have better machinability than alloy steels of comparable carbon content and hardness.

4.4 Heat Treatment of Steels

Practically all steel heat treatments involve heating into γ (austenite) region and then cooling back to ambient temperatures. The important variable in the heat treatment is the cooling rate, for this determines not only the size of the microstructure but also the nature of the phases present.

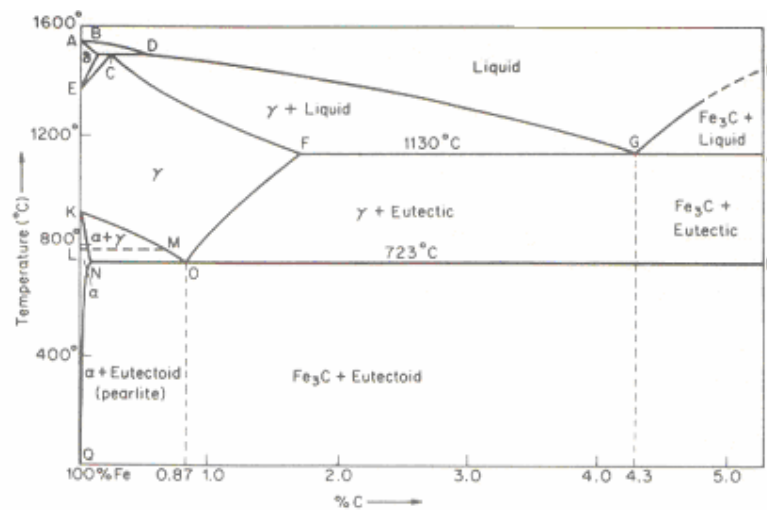
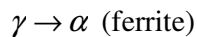


Figure 4.2: Iron-Carbon Phase Diagram [33]

By looking at Figure 4.2, there are three equilibrium phase transformations:



Ferrite is the name given to body centered cubic allotropes of iron and can be achieved by very slow cooling from austenitization range until complete transformation occurs. Ferrite is soft and gummy. Its carbon content is very low (0.021%) and can also be considered as pure iron.

Cementite is the name given to the carbide of iron. It is extremely hard and brittle due to high carbon content (6.67%). It has orthorombic crystal structure.

Pearlite is the eutectoid mixture of ferrite and cementite, and is formed when austenite decomposes during cooling. It consists of alternate thin layers, or lamellae, of ferrite and cementite.

Martensite is the name given to the very hard and brittle constituent that is formed when a steel is very rapidly cooled from the austenitic state. Austenite changes into a body centered lattice with all the carbon trapped in interstitial solid solution. The hardness of martensite depends on the carbon content, and is the greatest in high carbon steels.

John [33] states that, bainite is the term that is given to the decomposition product which is formed when austenite decomposes by either isothermal transformation, or at a cooling rate intermediate between the very rapid cooling necessary for martensite formation and the slower rate of cooling at which pearlite is formed.

By application of heat treatment procedures to steels, it is possible to achieve certain microstructures and thus mechanical properties. Cooling rate is the deciding factor for heat treatment. If slow, stable cooling procedure is applied, uniform phases, if fast and unstable cooling procedure is applied, non-uniform phases are achieved. Time-temperature-transformation curves (or T-T-T diagrams) are used for determination of the cooling procedure.

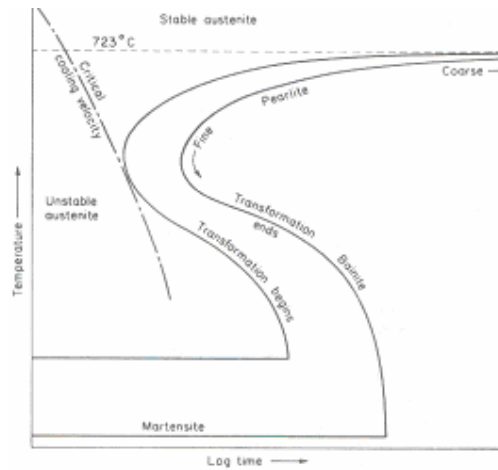


Figure 4.3: A Typical TTT Diagram for Plain Carbon Steels [33]

A typical T-T-T diagram for plain carbon steels is shown in Figure 4.3. A slow cooling rate will lead to the transformation of coarse pearlite, with little undercooling of austenite, while a faster cooling rate will give a greater amount of undercooling and the formation of pearlite. If the critical cooling velocity is exceeded, the non equilibrium phase, martensite will be formed. Bainite may be formed by the isothermal transformation of undercooled austenite.

Major heat treatment types are annealing, normalising and quenching but by varying the time or temperature parameters, many other treatments can be performed.

4.4.1 Annealing

For a given steel, the critical temperatures depend on whether the steel is being heated or cooled. Critical temperatures for the start and completion of the transformation to austenite during heating are denoted, respectively, by A_{c1} and A_{c3} for hypoeutectoid steels and by A_{c1} and A_{cm} for hypereutectoid steels. These temperatures are higher than the corresponding critical temperatures for the start and completion of the transformation from austenite during cooling, which are

denoted respectively, by A_{r3} and A_{r1} for hypoeutectoid steels and by A_{rcm} and A_{r1} for hypereutectoid steels. These critical temperatures converge to the equilibrium values A_{e1} , A_{e3} and A_{ecm} as the rates of heating or cooling become infinitively slow. Figure 4.4 illustrates the positions of A_{e1} , A_{e3} and A_{ecm} lines on the equilibrium phase diagram for plain carbon steels [34].

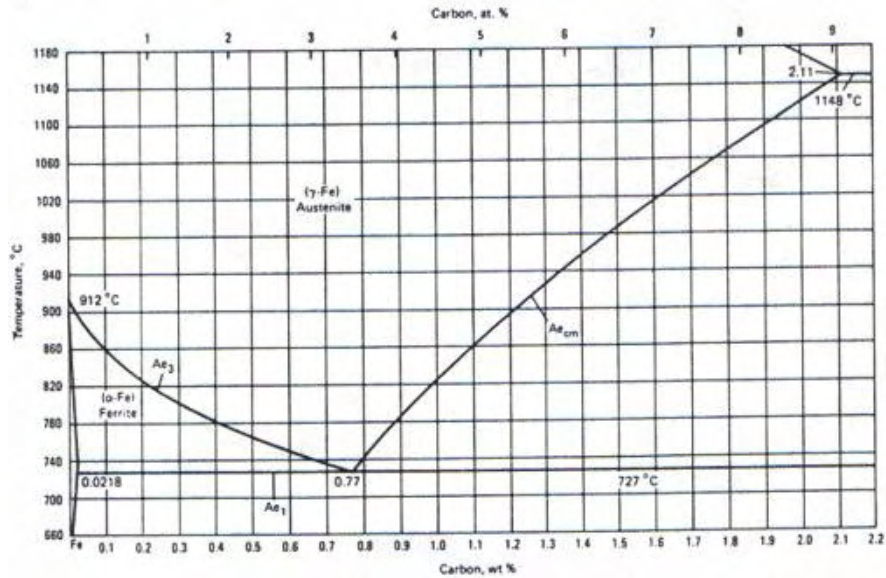


Figure 4.4: Fe-Fe₃C phase diagram showing the temperature range of interest for annealing plain carbon steels [34]

In practice, specific thermal cycles of an almost infinite variety are used to achieve the various goals of annealing. These cycles fall into several broad categories that can be classified according to the temperature to which the steel is heated and the method of cooling used. The maximum temperature may be below the lower critical temperature, A_1 (subcritical annealing); above A_1 but below the upper critical temperature, A_3 in hypoeutectoid steels or A_{cm} in hypereutectoid steels (intercritical annealing); or above A_3 (full annealing). Because some austenite is present at temperatures above A_1 cooling practice through transformation is a crucial factor in achieving desired microstructures and properties. Accordingly, steels heated above

A_1 are subjected either to slow continuous cooling or to isothermal treatment at some temperature below A_1 at which transformation to the desired microstructure can occur in a reasonable amount of time [34].

Subcritical annealing (below A_1) does not involve formation of austenite. In as rolled or forged hypoeutectoid steels containing ferrite and pearlite, subcritical annealing can adjust the hardness of both constituents, but excessively long times at temperature may be required for substantial softening. The subcritical treatment is most effective when applied to hardened or cold worked steels, which recrystallize readily to form new ferrite grains. The rate of softening increases rapidly as the annealing temperature approaches A_1 . Cooling practice from the subcritical annealing temperature has very little effect on the established microstructure and resultant properties [34].

Austenite begins to form when the temperature of the steel exceeds A_1 . In hypoeutectoid steels, the equilibrium structure in the intercritical range between A_1 and A_3 consists of ferrite and austenite, and above A_3 the structure becomes completely austenitic. However, the equilibrium mixture of ferrite and austenite is not achieved instantaneously. Undissolved carbides may persist, especially if the austenitizing time is short or the temperature is near A_1 , causing the austenite to be inhomogeneous.

The more homogeneous structures developed at higher austenitizing temperatures tend to promote lamellar carbide structures on cooling, whereas lower austenitizing temperatures in the intercritical range result in less homogeneous austenite, which promotes formation of spheroidal carbides [34].

Austenite formed when steel is heated above the A_1 temperature transforms back to ferrite and carbide when the steel is cooled below A_1 . The rate of austenite decomposition and the tendency of the carbide structure to be either lamellar or spheroidal depend largely on the temperature of transformation. If the austenite transforms just below A_1 , it will decompose slowly. The product then may contain

relatively coarse spheroidal carbides or coarse lamellar pearlite, depending on the composition of the steel and the austenitizing temperature. This product tends to be very soft. However, the low rate of transformation at temperatures just below A_1 necessitates long holding times in isothermal treatments, or very low cooling rates in continuous cooling, if maximum softness is desired. Isothermal treatments are more efficient than slow continuous cooling in terms of achieving desired structures and softness in the minimum amount of time.

As the transformation temperature decreases, austenite generally decomposes more rapidly, and the transformation product is harder, more lamellar and less coarse than the product formed just below A_1 [34].

After the austenite has been completely transformed, little else of metallurgical consequence can occur during cooling to room temperature. Extremely slow cooling may cause some agglomeration of carbides, and consequently, some slight further softening of the steel, but in this regard such slow cooling is less effective than high temperature transformation. Therefore, there is no metallurgical reason for slow cooling after transformation has been completed, and the steel may be cooled from the transformation temperature as rapidly as feasible in order to minimize the total time required for the operation [34].

Although the time at the austenitizing temperature may have only a small effect on actual hardness, its effect on machinability or cold forming properties may be appreciable. Long term austenitizing is effective in hypereutectoid steels because it produces agglomeration of residual carbides in the austenite. Coarser carbides promote a softer final product. In lower carbon steels, carbides are unstable at temperatures above A_1 and tend to dissolve in the austenite, although the dissolution may be slow [34].

4.4.2 Spherodizing

Steels may be spherodized—that is heated and cooled to produce a structure of globular carbides in a ferritic matrix—by the following methods:

- Prolonged holding at a temperature just below A_{e1} .
- Heating and cooling alternately between the temperatures that are just above A_{c1} and just below A_{r1} .
- Heating to a temperature above A_{c1} , and then either cooling very slowly in the furnace or holding at a temperature just below A_{r1} .
- Cooling at a suitable rate from the minimum temperature at which all carbide is dissolved, to prevent reformation of a carbide network, and then reheating in accordance with method 1 or 2 above (applicable to hypereutectoid steel containing a carbide network).

The rates of spherodizing provided by these methods depend somewhat on prior microstructure, being greatest for quenched structures in which the carbide phase is fine and dispersed. Prior cold work also increases the rate of the spherodizing reaction in a subcritical spherodizing treatment.

For full spherodizing, austenitizing temperatures either slightly above the A_{c1} temperature or about midway between A_{c1} and A_{c3} are used. If a temperature slightly above A_{c1} is to be used, good loading characteristics and accurate temperature controls are required for proper results; otherwise, it is conceivable that A_{c1} may not be reached and thus that austenitization may not occur. Because time and temperature affect austenitization and thereby influence the number of undissolved carbides from which nucleation and coalescence of the spheroids occur, close control of temperature is necessary. For example, if it is determined that spherodization of a given steel will require an austenitizing temperature of

750°C, a deviation of 11°C may easily result in an incompletely spherodized structure.

The spherodized structure is desirable when minimum hardness, maximum ductility or (for high carbon steels) maximum machinability is important. Low carbon steels are seldom spherodized, for machining, because in the spherodized condition they are excessively soft and 'gummy', cutting with long, tough chips. When low carbon steels are spherodized, it is generally to permit severe deformation. For example, when 1020 steel tubing is being produced by cold drawing in two or three phases, a spherodized structure will be obtained if the material is annealed for ½ to 1 h at 690°C after each pass. The final product will have a hardness of about 163 HB. Tubing in this condition will be able to withstand severe deformation during subsequent cold forming.

As with many other types of heat treatment, hardness after spherodizing depends on carbon and alloy contents. Increasing the carbon or alloy content, or both, results in an increase in the as-spherodized hardness, which generally ranges from 163 to 212 HB [34].

CHAPTER V

SOUND VELOCITY

5.1 Introduction

Sound waves are elastic waves and they can be transmitted through both fluid and solid media. The audible range of frequency is from about 20 Hz to about 20 kHz. Elastic waves with frequencies higher than the audio range are described as ultrasonic. The waves used for the non-destructive inspection of materials are usually within the frequency range of 0.5 MHz to 20 MHz. Most significant aspect of ultrasonic waves are their much higher frequency. With this property, they can be reflected off defects inside the materials and it is this characteristic which makes them important tool for defect detection. Ultrasonic waves consist of oscillations or vibrations of the atomic particles about the equilibrium positions.

Ultrasonic material analysis is based on a simple principle of physics: the motion of any wave will be affected by the medium through which it travels. Thus, changes in one or more of four easily measurable parameters associated with the passage of a high frequency content-can often be correlated with changes in physical properties such as hardness, elastic modulus, density, homogeneity, or grain structure. General application areas of ultrasonic testing are flaw detection, thickness gauging, bond characteristics determination. By ultrasonic methods, microstructural, compositional changes can be detected which leads to changes in some basic mechanical properties such as hardness and elastic modulus [35].

Sonat [36] states that, ultrasonic techniques are widely used for the detection of internal defects in materials, but they can also be used for the detection of small

surface cracks. Major advantage of ultrasonic testing is that, it can be used for testing the most materials. Another important advantage is that the techniques are also in regular use for the in-service testing of parts and assemblies. Ultrasonic testing is being used for more than 40 years in industry. Today it is expected that ultrasonic testing, supported by great advances in instrument technology, give reproducible test results within narrow tolerances.

5.2 Sound Velocity

By means of ultrasonic velocity measurement, elastic moduli, and some mechanical and microstructural changes in solids can be determined. These changes affects mechanical properties of materials such as hardness, impact toughness etc. So it is likely to have a correlation between ultrasonic velocity changes and some mechanical properties like hardness and these correlations must be further investigated in order to broaden the use of these techniques.

In fluids, sound velocity is defined as:

$$V = \left(\frac{\kappa}{\rho} \right)^{1/2} \quad (5.1)$$

where,

κ : Bulk stiffness modulus,

ρ : Density

In solid medium, due to shear elasticity and presence of boundaries, the situation is more complicated. Elastic properties of medium and relative size of the object affects wave propagation properties.

If the particle motion in a wave is along the line of the direction of travel of the wave, the resulting wave is called a **longitudinal** wave (compression wave). Such waves can be propagated in solids, and liquids. Longitudinal waves are easily generated and often used in ultrasonic testing.

Bozay [37] states that, sound propagation is caused by the elastic bond between the particles, wherein each particle as it moves from its equilibrium position pushes or pulls the adjacent particles, which then in turn transmit this energy on to the next adjacent particles and so on. Almost all of the sound energy used in ultrasonic testing originates as longitudinal sound and then may be converted to the other modes for special test applications.

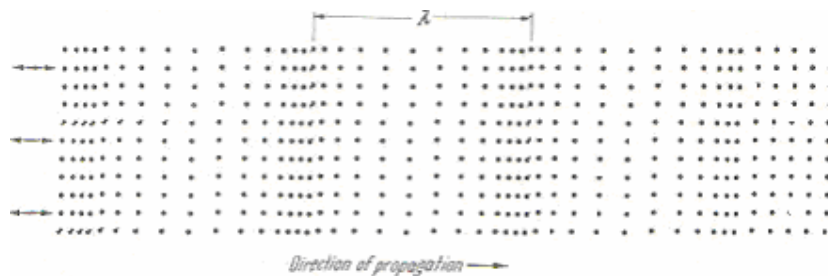


Figure 5.1: Longitudinal Wave [48]

In solid materials it is possible, also, for the particle movement to be at right angles to the direction of travel of the wave, and such waves are called **shear** waves. These usually have a velocity of approximately half of that of longitudinal waves in the same material and for practical purposes cannot be generated in liquids and gases.

These waves exist, for all practical purposes, only in solids because the distance between molecules, the mean free path, is so great in liquids and gases that the attraction between particles is not sufficient to allow one particle to move another more than a fraction of its own movement, so the wave is rapidly attenuated [37].

According to Smith [38], for this wave to travel through a material it is necessary that each particle show sufficient attraction on the adjacent particles so that as one particle moves, pulls its neighbor with it. As a result of their slower speeds shear waves have shorter wavelengths than same frequency of longitudinal waves.

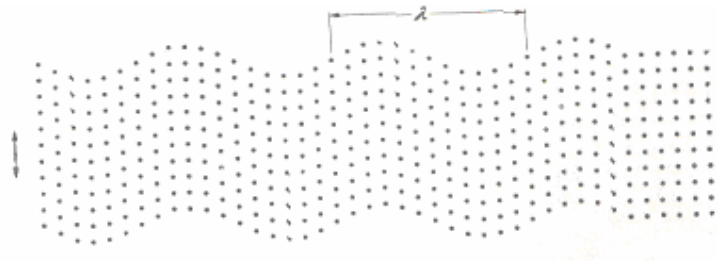


Figure 5.2: Transverse Wave [48]

Surface waves can be generated on the free surface of any solid material. They are somewhat analogous to water waves in which the motion of particles is both transverse and longitudinal in a plane containing the direction of propagation and the normal to the surface. In surface waves the particle movement is elliptical and such waves exist only in the surface layer of solids [2].

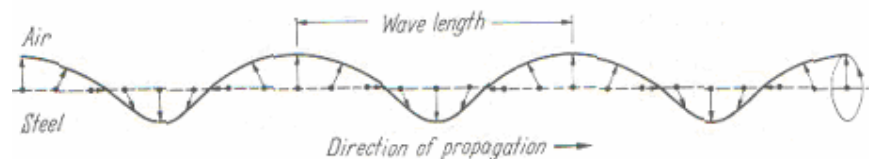


Figure 5.3: Surface Wave on Steel [48]

When ultrasonic waves are generated in a relatively thin solid substance whose thickness is less than one wavelength, a pure surface wave cannot exist, and a complex vibration occurs throughout the material thickness. Their velocities

through a material are dependent not only on the type of material, but on the material thickness, the frequency of the sound wave, and its mode and type [37].

For longitudinal waves, in a specimen of large dimensions compared to the wavelength:

$$V_L = \left(\frac{E \cdot (1 - \nu)}{\rho \cdot (1 + \nu) \cdot (1 - 2\nu)} \right)^{1/2} \quad (5.2)$$

where,

E : Young's modulus (MPa),

ρ : Density (kg/m³),

ν : Poisson's ratio

The shear velocity is given by:

$$V_T = \left(\frac{G}{\rho} \right)^{1/2} = \left(\frac{E}{2\rho(1 + \nu)} \right)^{1/2} \quad (5.3)$$

where,

G : Shear modulus (MPa),

ρ : Density (kg/m³)

Surface (Rayleigh) wave velocity is given by

$$V_R = 0.9 \cdot V_T \quad (5.4)$$

The velocity is influenced by the microstructure of a polycrystalline material through changes in the moduli of the individual grains, through orientation of the grains by texture, through second phases that modify metal stiffness, and through energy absorption mechanisms that generally lower the moduli in certain frequency and/or temperature ranges. For homogenous isotropic polycrystals, the elastic

wave/vibration quantities can be predicted approximately from single-crystal data by the theories of Voigt et.al. For homogenous polycrystals that have been rolled or drawn into perfectly oriented textures, the elastic properties reduce to the crystal properties themselves. For intermediate textures, the elastic parameters cannot be predicted quantitatively. However, it can be said that the parameters are somewhere between their values for the single crystals and for the isotropic polycrystals [4].

The velocity of an ultrasound (c) is given as:

$$c = f \cdot \lambda \quad (5.5)$$

in a perfectly elastic material and at constant temperature and pressure.

where,

c :Sound velocity (m/s),

f :Frequency (s^{-1}),

λ :Wavelength (m)

Frequency is the number of cycles completed in one second and is measured in Hertz (Hz). The time required to complete full cycle is period, it is the reverse of the frequency and measured in seconds.

$$f = \frac{1}{T} \quad (5.6)$$

So velocity equation can also be written as:

$$c = \frac{\lambda}{T} \quad (5.7)$$

where,

c : Sound velocity (m/s),

T : Period (s),

λ : Wavelength (m)

Sound velocity is a function of the tested material. It changes from material to material and also some internal changes in the material affects the sound velocity. This property is very useful in order to correlate some mechanical property changes with sound velocity.

Table 5.1: Ultrasonic velocities in various media (mean values) [48]

Material	Relative Density (g/cm³)	Longitudinal Wave Velocity (m/s)	Shear Wave Velocity (m/s)
Aluminium	2.70	6300	3080
Mild Steel	7.85	5900	3230
Magnesium	1.70	5770	3050
Copper	8.90	4700	2260
Titanium	4.51	6000	3000
Polythene	1.20	2000	540
Perspex (Lucite)	1.18	2700	1300
Water	1.00	1490	-
Air	-	344	-

5.3 Sound Velocity Measurement by Pulse-Echo System

In pulse-echo inspection, short bursts of ultrasonic energy (pulses) are introduced into a test piece at regular intervals of time. If the pulses encounter a reflecting surface, some or all of the energy is reflected. The proportion of energy that is reflected is highly dependent on the size of the incident ultrasonic beam. The direction of the reflected beam depends on the orientation of the reflecting surface with respect to the incident beam. Reflected energy is monitored; both the amount

of energy reflected in a specific direction and time delay between transmission of the initial pulse and receipt of the echo are measured [39].

According to Green [40] and Keleş [41], in pulse-echo testing method, ideally the test object must have smooth, flat, parallel opposing surfaces. In addition, sufficient force on the transducer is required to squeeze out excess couplant between it and the test object. The ultrasonic measuring technique is comparative, i.e., there exist always references and the measurements are evaluated with respect to these references.

The main principle of ultrasonic velocity measurement is as follows: an ultrasonic wave is sent into the test material with the help of either longitudinal or transverse probes and the reflection of these waves are collected. By measuring the distance travelled by these waves and time passed for this travel, it is possible to determine the ultrasonic velocity in that material. Ultrasonic velocity is a function of material and it is possible to distinguish for example steel from aluminium, magnesium titanium etc. thus all has specific sound velocity values.

In sound velocity determination, travelled distance is mostly the thickness for plate like objects and it can be measured by micrometers with very high accuracies up to 0.01 % when surfaces are smooth and measurement is made very carefully. After determination of thickness, next point is the measurement of time for the travel of the ultrasonic wave. Again, it can be measured very precisely because measurements are in the order of microseconds. Once these measurements are made, ultrasonic velocity can be found from the equation

$$c=2\frac{T}{t_s} \quad (5.8)$$

where,

T : Material thickness (m),

c : Sound velocity (m/s),

t_s : Measured time (s)

CHAPTER VI

EXPERIMENTAL PROCEDURE

6.1 Workpiece Characteristics

AISI/SAE 1040 and 1050 steels which were used in this study, were obtained from ASİL ÇELİK-Bursa in the hot-rolled bar form. SAE 1040 and 1050 are the mostly used and easily achieved typical medium carbon steels in the market. Production history of the round bars is, steel production in EAF, vacuum degassing, continuous casting, reheating, de-scaling, continuous rolling, cooling in air, shot blasting, and straightening. Specimens have dimensions of 125 mm in length and 75 mm in diameter. For experimental purposes, 16 specimens obtained, 8 of them were SAE 1040 and 8 of them were SAE 1050. As a first part of the study, spectrometric analysis of the steels were performed and obtained results are given in the Table 6.1.

Table 6.1: Chemical composition analysis of the workpieces

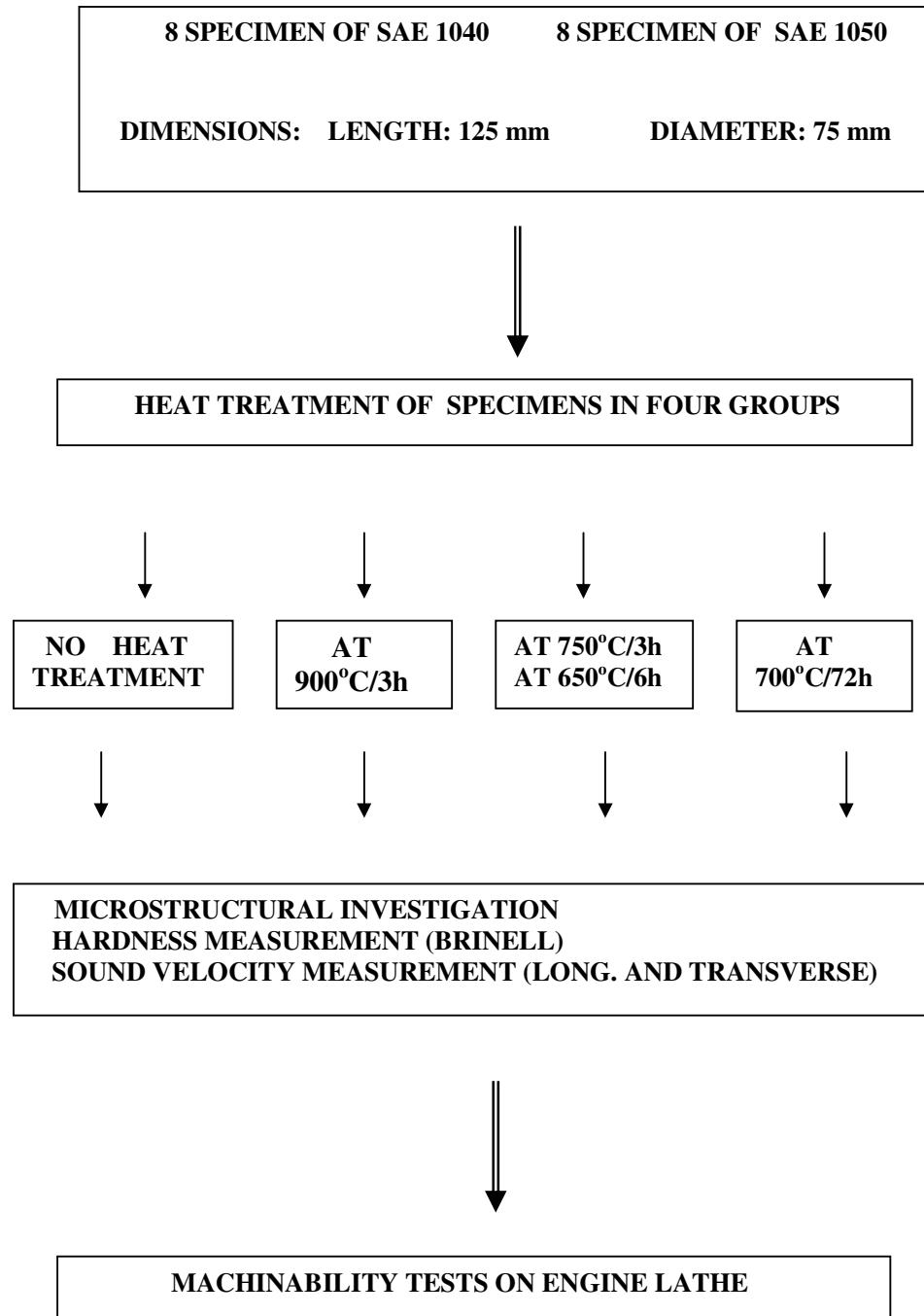
Steel	C%	Mn%	Si%	P%	S%	Al%
SAE 1040	0.38-0.40	0.6-0.9	0.20-0.35	Max. 0.03	Max. 0.04	Max. 0.019
SAE 1050	0.47-0.50	0.6-0.9	0.25-0.35	Max. 0.03	Max. 0.04	Max. 0.019

Average mechanical properties of SAE/AISI 1040 and 1050 steels are as follows:

Table 6.2: Average mechanical properties of the workpieces [34]

Steel	Tensile Strength (MPa)	Yield Strength (MPa)	Elongation (%)	Reduction in Area (%)	Hardness (Brinell)
SAE 1040	589.5	374	28	54.9	170
SAE 1050	748	427	20	39.4	210

6.2 Flow-Chart of the Study



6.3 Preliminary Studies:

As a first step, a cross section of 10 mm thickness were cut from one of the SAE 1040 and 1050 steels for preliminary examinations. On these pieces, hardness measurements were performed and it was seen that hardness values on the entire surface show no difference more than 5% which is acceptable. Details of the hardness measurement and related results will be given in the following sections.

On these pieces, metallographic examinations were also performed and for both steel types expected microstructures were observed. Details of the microstructural examination and photographs will also be given in the following sections.

As a last preliminary study, ultrasonic sound velocities were measured on various parts of the specimen surfaces and it was seen that both steel types have uniform structures and no inhomogeneity or flaws present, thus all ultrasonic velocity values were very close to each other.

6.4 Heat Treatment of the Workpieces

As stated before, there were 16 specimens used, 8 of which were SAE 1040 and 8 of which were SAE 1050. Both SAE 1040 and 1050 workpieces were divided into four groups and three different heat treatment procedures applied on them. One group was not heat treated and it was left as reference group.

Recalling from section 4.4.2, spherodized structure in steels can be achieved by:

- 1) Prolonged holding at a temperature just below A_{e1} .
- 2) Heating and cooling alternately between the temperatures that are just above A_{c1} and just below A_{r1} .

- 3) Heating to a temperature above A_{c1} , and then either cooling very slowly in the furnace or holding at a temperature just below A_{r1} .
- 4) Cooling at a suitable rate from the minimum temperature at which all carbide is dissolved, to prevent reformation of a carbide network, and then reheating in accordance with method 1 or 2 above (applicable to hypereutectoid steel containing a carbide network).

First heat treatment procedure was selected as annealing which is performed by heating the specimen up to the single phase γ region and then cooling very slowly. Details of this treatment were discussed in the section 3.4.1.

Second heat treatment procedure was selected as heating to a temperature above A_{c1} , and then cooling below A_{r1} . It was mentioned before that, the more homogenous structures developed at higher austenitizing temperatures tend to promote lamellar carbide structures on cooling, whereas lower austenitizing temperatures in the intercritical range result in less homogenous austenite, which promotes formation of spheroidal carbides.

Third heat treatment procedure is selected as prolonged holding at a temperature just below A_{e1} . This treatment is the most common spheroidizing treatment.

Before proceeding further, it is necessary to define the critical temperatures for both AISI/SAE 1040 and 1050 steels.

Table 6.3: Approximate critical temperatures for workpieces [34]

Steel	A_{c1} ($^{\circ}C$)	A_{c3} ($^{\circ}C$)	A_{r3} ($^{\circ}C$)	A_{r1} ($^{\circ}C$)
SAE 1040	721	793	757	671
SAE 1050	721	768	741	682

On very slow cooling rates, Ac_1 converge to equilibrium value Ae_1 . With these information, it is possible to determine the temperatures of the corresponding heat treatments.

First heat treatment group is annealing and for performing this, specimens were heated to single phase γ region and cooled in furnace. For this purpose, both specimen types were heated to 900°C , kept at this temperature for 3 h and then cooled in the furnace.

Second heat treatment group requires heating above Ac_1 temperature, cooling back under the Ar_1 temperature and keeping the specimen at this temperature for a definite period (isothermal treatment). Ac_1 temperature for both SAE 1040 and 1050 steels are 721°C . So heating temperature was selected as 750°C . By looking at Table 6.3, it can be seen that Ar_1 temperature for 1040 steel is 671°C and for 1050 steel is 682°C . For both steel types, suitable temperature was selected as 650°C . After determining the temperatures, it is necessary to define waiting times. After several trials optimum parameters were achieved. These were: heating to 750°C and keeping the specimen at that temperature for 3 h, and then cooling back to 650°C in furnace and keeping the specimen at that temperature for 6 h for isothermal treatment.

Last heat treatment group is prolonged holding at a temperature just below Ae_1 (Ac_1). For both SAE 1040 and 1050 steels, Ae_1 temperature is 721°C . With these information, last heat treatment procedure is as follows: Heating to 700°C and waiting at that temperature for a prolonged period. References stated that waiting duration for these treatment generally above 24 h and increases with the dimensions of the workpieces. Since specimen diameter was considerably large, a couple of trials were performed on previously cutted specimens. By microstructural analysis, it was seen that specimens which are kept at 700°C for 72 h gives fully spherodized microstructure.

All the heat treatments were performed at METU Metallurgical & Materials Engineering Department Heat Treatment Laboratory.

Table 6.4: Summary of applied heat treatments

Steel	Code	Threatment History
AISI/SAE 1040	A₀	No Heat Treatment
	A₁	900°C/3h/FC*
	A₂	750°C/3h- 650°C/6h/FC*
	A₃	700°C/72h/FC*
AISI/SAE 1050	B₀	No Heat Treatment
	B₁	900°C/3h/FC*
	B₂	750°C/3h- 650°C/6h/FC*
	B₃	700°C/72h/FC*

*Furnace Cooling

6.5.Metallographic Analysis of the Wokpieces:

Metallographic examinations were performed in order to analyse the developed microstructures of the workpieces as a result of applied heat treatments. In order to be able to perform metallographic analysis, samples were taken from each specimen, with 10 mm thickness. After this, all these specimens were cut into four pieces in order to examine them under the microscope easily.

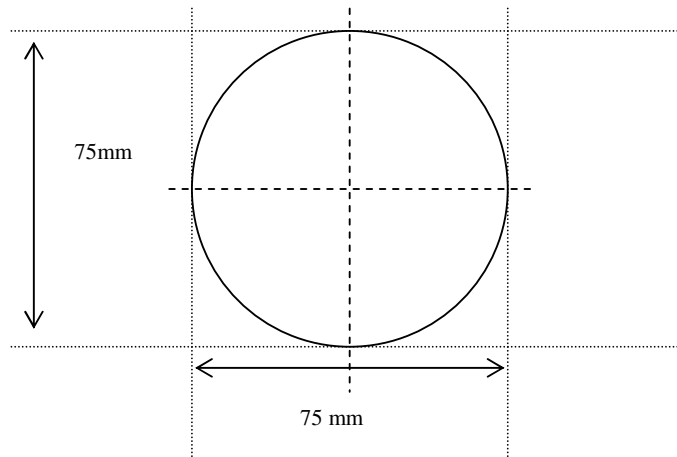


Figure 6.1: Top-view of the cutted specimen

For having a good microstructural image under microscope, specimens were prepared carefully. As a first step, specimen surfaces were grinded with silicon carbide (SiC) abrasive papers. There were different abrasive papers having different mesh numbers of 220, 320, 400, 500, 600, 800 and 1200. Grinding operation was started from low mesh numbers and continued with each next higher mesh numbered paper. This operation was done under running water in order to eliminate the effect of heat that produced as a result of friction during grinding. After grinding, specimens were polished with rotating $1 \mu\text{m}$ Al_2O_3 powder in order to eliminate scratches produced during grinding. As a last step, specimens were etched, that is immersed into a 2% H_2O_3 (Nital) solution for about 5 seconds and then immediately washed and dried. Microstructural analyses were performed with BHMT Olympus optical microscope and representative photomicrographs were taken with Nikon Optihot type optical microscope. All the metallographic investigations were performed at M.E.T.U Metallurgical & Materials Engineering Department Metallography Laboratory.

6.6 Hardness Test of the Workpieces

Most of the mechanical properties of steels can be related to their hardness values, as well as microstructure. Hardness can be defined as a resistance of a metal to indentation. If hardness value of a metal is high, it means that it is more difficult to deform it plastically. Hardness tests are very simple, only small indentation on the specimen surface is created and its dimensions or depth are measured. Since created indentation is very small and material is not deformed or fractured, hardness test is different from the other destructive mechanical tests like tension test during which metal is plastically deformed and then fractured.

There are different hardness value representations. Most commonly used hardness representations are Brinell, Rockwell and Vickers. These values can be converted into each other.

In order to make comparisons with the previous investigations, Brinell hardness test was preferred. This test utilizes a hardened steel ball indenter of 10 mm diameter forced into the surface of the metal being tested under a static load of 3000 kg and the load maintained for 10-15 seconds. The Brinell hardness number, HB, is given by:

$$H_B = \frac{\text{applied load (kg)}}{\text{surface area of the impression (mm}^2\text{)}} \quad (6.1)$$

Hardness tests were performed at METU Metallurgical and Materials Engineering Department Mechanical Test Laboratory. Utilized device was VEB Werkstoffprof Machine. On each specimen, three hardness measurements were performed, one from center, one from mid-point between center and edge and one from a point closer to the edge, see Figure 6.1. Average of these three measurements was taken as hardness value.

6.7 Ultrasonic Velocity Measurement of the Workpieces

Ultrasonic velocity measurements were performed with Panametrics-5052UAX50 analyzer. Both longitudinal and transverse wave velocities were measured. Longitudinal wave velocities were measured with probes having frequencies 5 MHz (Panametrics V109 5.0/0.5 149548) and 10 MHz (Panametrics V111 10.0/0.5, 142275), transverse wave velocities were measured with the probe having frequency 5 MHz (Panametrics V155 79278, 5.0/0.5). These probes are contact type 12.6 mm diameter piezoelectric disc.

In the measurements, pulse-echo technique was used. A constant force was applied to the probe against the specimen surface to have constant layer at surface/probe contact. In longitudinal wave velocity measurement, machine oil was used as couplant and semisolid lemon was used in transverse wave velocity measurement. In velocity measurement, as it was mentioned before, an ultrasonic wave was send into the test material with the help of either longitudinal or transverse probes and the reflection of these waves were collected. By measuring the distance travelled by these waves and time passed for this travel, it was possible to determine the ultrasonic velocity in that material. In the case of this study, distance was the thickness of the specimens and was measured with micrometers. Accuracy of these micrometers is between 0.1-0.01 %. With the testing instrument, it was possible to measure the time taken for the ultrasonic waves to travel through thickness of the material. Measurements were performed in microseconds and accuracy of these measurements were about $\pm 2 \mu\text{s}$. Ultrasonic velocity could be found from the equation $c = 2T/t$, where T is specimen thickness, t is time of flight and c is the velocity of the wave in the specimen.

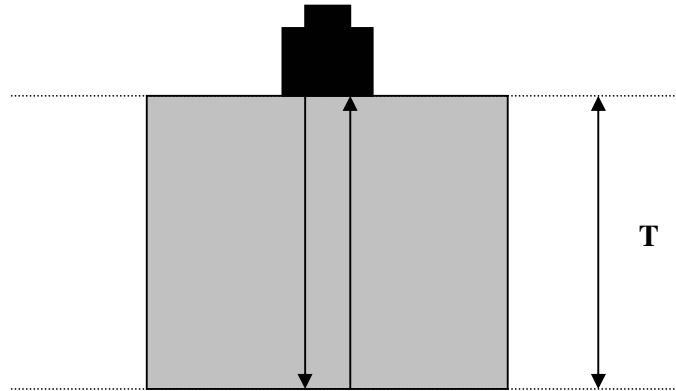


Figure 6.2: Illustration of the ultrasonic wave travel

On measuring the time, the interval between 2nd and 3rd echoes was taken. As a reference, the points at which they become positive for the second time are taken. For each specimen group, four different measurements were taken. All these measurements and standard deviations of these measurements will be given in the next chapter. Differences between measurements were within the accuracy range. These differences occurred due to: surface roughness, small variations in specimen thickness and surface parallelity.

6.8 Machinability Testing

6.8.1 Specification of the Engine Lathe:

Turning operations were performed at the Mechanical Engineering Department Workshop. ÖRNMASKINER Storebro (Sweden) engine lathe was used for this purpose. It has spindle speed ranges of 25, 36, 50, 70, 100, 140, 200, 285, 400, 565, 800 and 1130 rpm.

6.8.2 Specification of the Workpieces:

In this study, 8 SAE 1040 and 8 SAE 1050 steel bars with 75mm diameter and 125 mm length were used. Two of SAE 1040 steel bars and two of SAE 1050 steel bars were not heat treated and used as a reference workpieces. To the rest of the bars, heat treatments applied, details of which were discussed in previous chapters. All heat treatment groups include 2 workpieces.

In the ISO 3685 standard, it is stated that length/diameter ratio should not be more than 10 (for these workpieces ratio is less than 2). Again, according to standard, hardness over complete cross-section should be within $\pm 5\%$. Hardness distribution on workpiece surfaces showed that, variations were within the limits. Last point is the necessity of the x100 and x500 magnification photomicrographs. These photographs were taken and will be presented in the following chapter.

6.8.3 Specifications of the Cutting Tool

During cutting operations, MTE 12x12x12 HSS Co T2 tools were used. For H.S.S tools, necessary tool geometry for this test is given in ISO 3685:1993 (E) tool life testing with single-point turning tools standard as:

Table 6.5: Necessary tool angles for standard tool life test [25]

Rake Angle (γ)	Clearance Angle (α)	Cutting Edge Inclination (λ_s)	Cutting Edge Angle (K_R)	Included Angle (ϵ_R)
25°	8°	0°	75°	90°

6.8.4 Cutting Operations

6.8.4.1 Preliminary Studies

As a starting operation, 6 mm central holes were drilled on workpieces for fixing them on lathe. Distance from corner of the tool to front of the lathe tool post holder was adjusted as 25 mm as stated in the ISO 3685 standard. Cutting edge on tools had no burrs or feather edge as stated in the standard. All cutting tools were examined before tests with a magnification of x10 for visual defects such as chips or cracks. With a different tool, a pass of about 2 mm has been removed in order to eliminate oxide, dirt on workpiece surfaces. No cutting fluid was used during cutting operations.

6.8.4.2 Cutting Parameters

Since all cutting variables affects machinability properties in some manner, all the parameters except cutting velocity were kept constant.

Table 6.6: Cutting parameters used in tool life tests

Spindle Speed	Feed (mm/rev)	Depth of Cut (mm)	Workpiece Diameter (mm)	Corner Radius (mm)
285 rpm	0.1	1	75	0.4

Since cutting velocities cannot be directly arranged on engine lathe, they are calculated by using the following formula:

$$S = \frac{\pi \cdot d_f \cdot (rpm)}{1000} \quad (6.2)$$

where,

- S : Cutting speed (m/min),
 d_f : Work diameter (mm),
 rpm : Spindle speed (revolution per minute)

In order to eliminate the effect of spindle speed, it was kept constant at 285 rpm and two different cutting velocities are achieved by changing the diameter of the workpiece. First cutting velocity 65.36 m/min is achieved according to formula 6.2 by reducing the workpiece diameter to 73 mm. Second cutting velocity of 53.72 m/min is achieved by reducing the workpiece diameter to 60 mm.

Table 6.7: Cutting velocities for different workpiece diameter at 285 rpm spindle speed

Cutting Velocity (m/min)	Workpiece Diameter (mm)
65.36	73
53.72	60

6.8.4.3 Tool Wear Measurement

Tool wear measurement was the most critical stage of this study, thus all the data needed for comparison of the relative machinabilities was obtained from tool wear vs. time graphics.

After the tool has been installed, cutting operation was performed for a definite time period (in this study, 4 min for cutting velocity of 53.72 m/min, and 2 min for cutting velocity of 65.36 m/min) and then cutting operation was interrupted. Tool was unfastened from the tool holder and all the sticking chip, workpiece or other residual particles removed without touching to the wear land. After this step, tool was placed under microscope with some inclination in order to coincide the wear land with the horizontal lines seen on microscopic view of the tool. By doing this, rake face of the tool becomes parallel to the lens. Wear on the flank land was

measured. Details of the flank wear land were given in the previous section 3.2.3. Since flank region was regularly worn, criteria for tool life was selected as average width of flank wear land $VB_B = 0.3$ mm. Each measurement was performed three times and average value was taken. After measurement has been taken, tool was taken to the engine lathe, installed to the tool post and cutting operation was continued for another definite period. This operation was continued until the flank wear criterion was achieved.

CHAPTER VII

RESULTS AND DISCUSSION

7.1 Introduction

This chapter includes, photomicrographs of the workpieces, results of the hardness measurements, results of the longitudinal and transverse ultrasonic wave velocity measurements and results of the tool wear measurements. Correlation of these measurements with each other is also given and represented graphically.

7.2 Photomicrographs of Workpieces

Metallographically prepared specimens were analyzed with the optical microscope. Entire specimen surfaces were analyzed and it was seen that microstructures were homogenous throughout the whole surface. Photomicrographs were taken with x100 and x500 magnification.

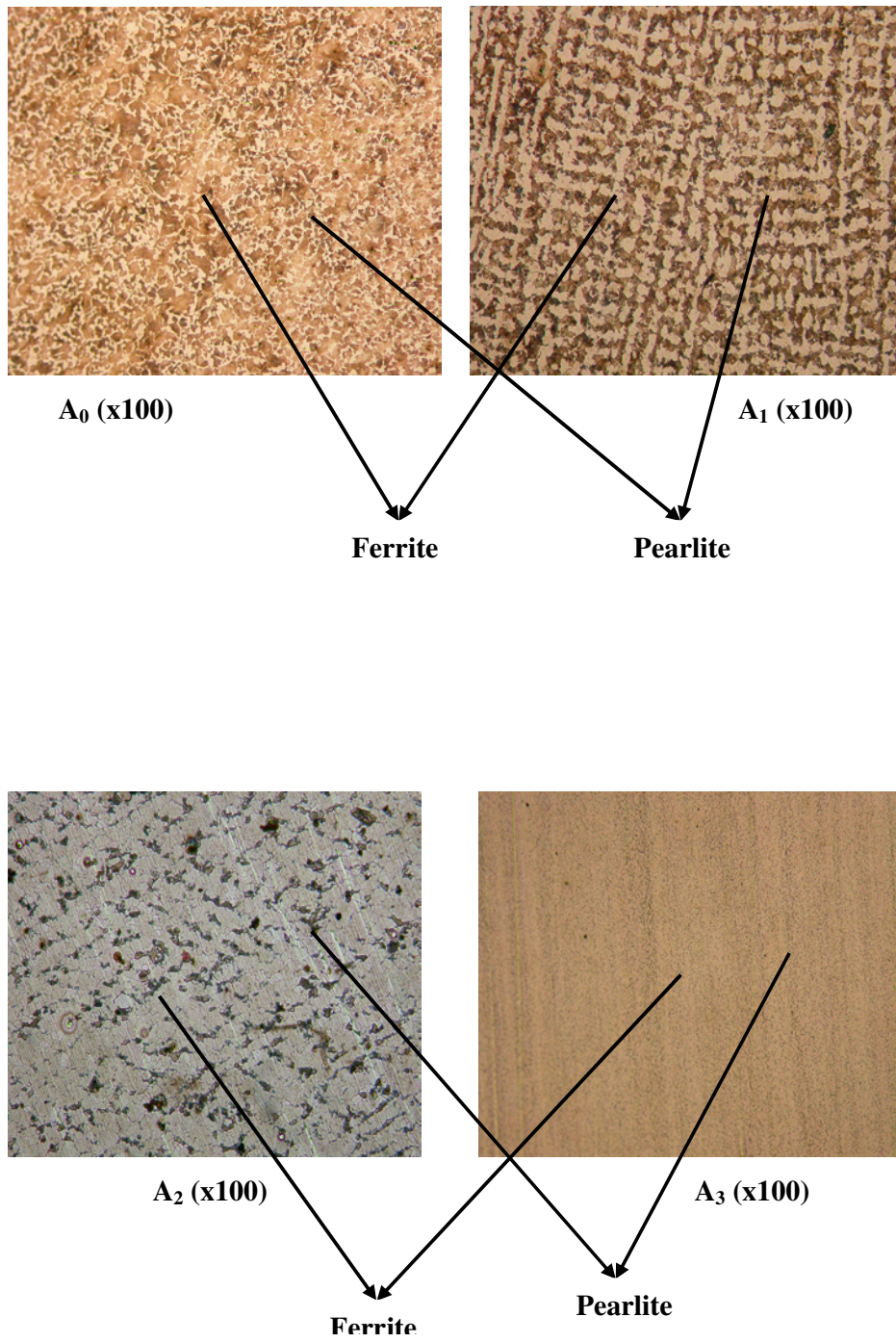


Figure 7.1: Photomicrographs of SAE 1040 specimens (with x100 magnification)

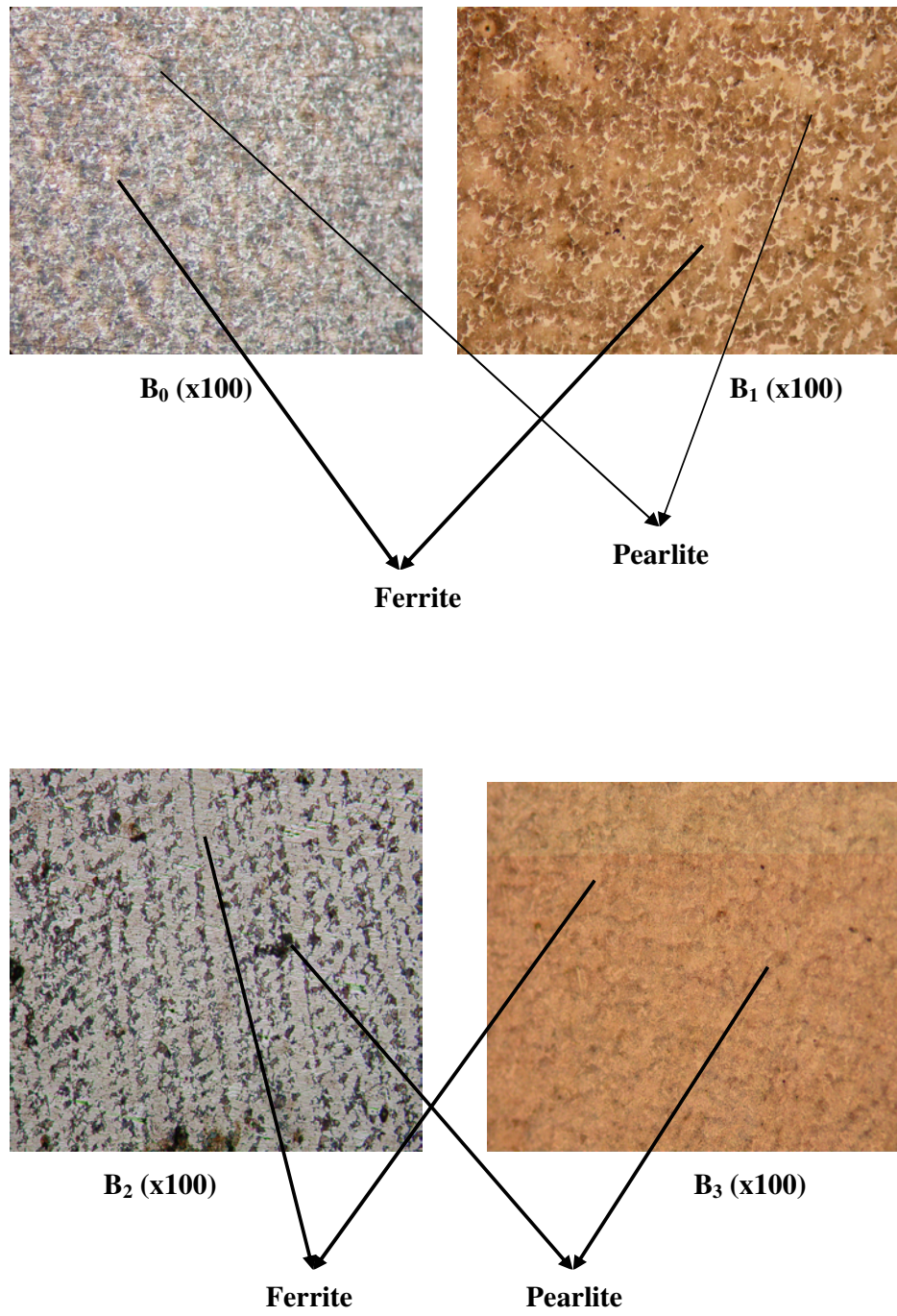


Figure 7.2: Photomicrographs of SAE 1050 specimens (with x100 magnification)

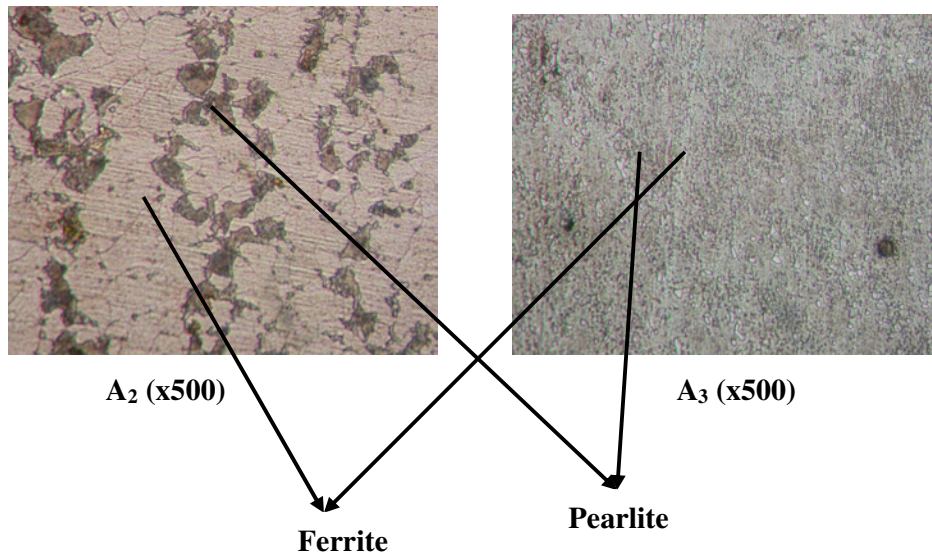
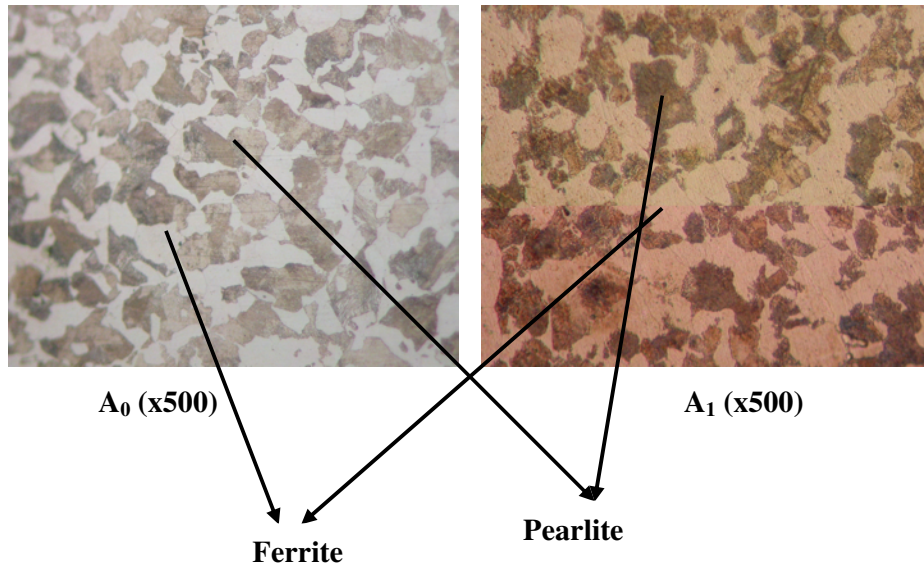


Figure 7.3: Photomicrographs of SAE 1040 specimens (with x500 magnification)

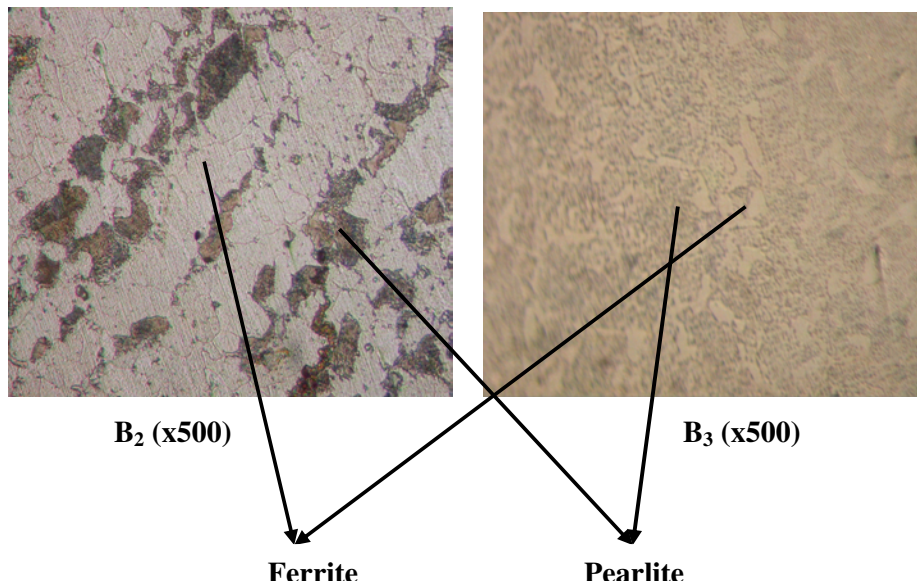
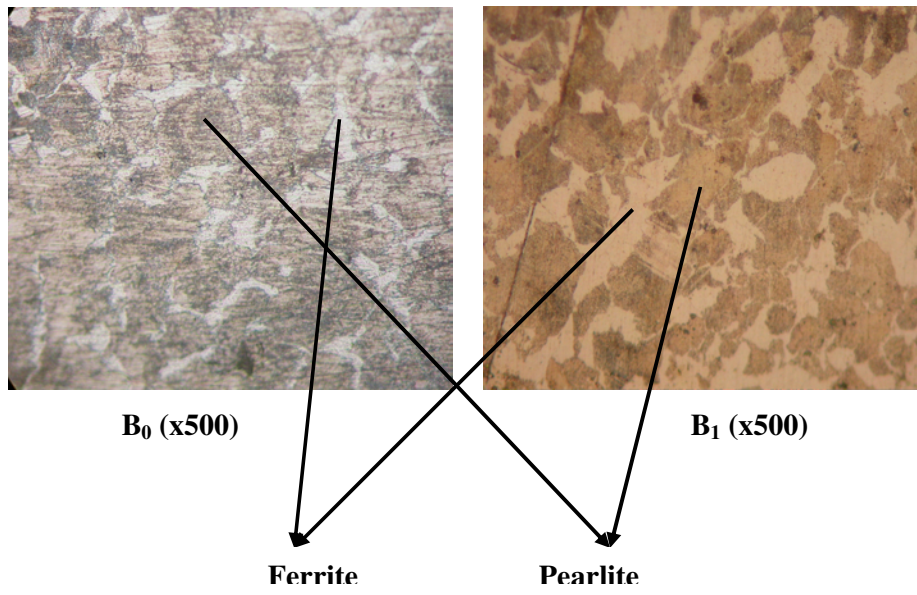


Figure 7.4: Photomicrographs of SAE 1050 specimens (with x500 magnification)

For the case of non-heat treated steel specimens (A_0 and B_0), ferritic and pearlitic structures were observed. Pearlitic regions can be seen as dark regions than ferritic regions can be seen as light regions. As can be seen from the microstructures, pearlite amount in the B_0 specimen is more than A_0 specimen. It is an expected result thus, as carbon content increases in the steel structure, pearlite amount increases. From iron-carbon phase diagram, ferrite and pearlite fractions in both steels can be calculated by the lever rule. With these calculations it was found that: A_0 has 50% ferrite, 50% pearlite and B_0 has 38% ferrite, 62% pearlite.

In the case of annealed steels (A_1 and B_1), it can be seen that grains are larger than the non-heat treated steel specimens for both steel types. It is also an expected result, thus annealing treatment leads to an increase in the grain sizes. In the case of A_1 specimen, a lamellar structure is observed but for B_1 specimen, structure is seen as fairly uniform.

As can be seen from the photomicrographs, both A_2 and B_2 specimens have lamellar pearlitic structures. For the case of B_2 specimen, this lamellar structure can be observed very clearly. With higher magnification, it is observed that structure also contains small amount of spherodites.

For the case of fourth heat treatment group, it can be seen that both A_3 and B_3 specimens have fully spherodized structures. Since B_3 specimen has more carbon content, spherodites are observed as larger than that of A_3 specimen.

7.3 Results of the Hardness Measurements of the Workpieces:

In this section, results of the hardness measurements are listed and also presented graphically. On the graphics, numbers on the x-axis represents corresponding heat treatments.

Table 7.1: Numbers representing corresponding heat treatments

Number	Heat Treatment History
1	No Heat Treatment
2	900°C/3h-FC*
3	750°C/3h-650°C/6h-FC*
4	700°C/72h-FC*

* Furnace Cooling

Table 7.2: Hardness values of SAE 1040 workpieces

Steel	Specimen Code	Heat Treatment History	Measurement Number	Hardness Values (Brinell)	
AISI/SAE 1040	A ₀	No Heat Treatment	1	179	
			2	176	
			3	176	
	AVERAGE HARDNESS of A ₀				177
	A ₁	900°C/ 3h/ FC*	1	150	
			2	144	
			3	141	
	AVERAGE HARDNESS of A ₁				145
	A ₂	750°C/ 3h & 650°C/ 6h/FC*	1	160	
			2	158	
			3	154	
	AVERAGE HARDNESS of A ₂				157
	A ₃	700°C/ 72h/ FC*	1	129	
			2	124	
			3	123	
	AVERAGE HARDNESS of A ₃				125

* Furnace Cooling

Table 7.3: Hardness values of SAE 1050 workpieces

Steel	Specimen Code	Heat Treatment History	Measurement Number	Hardness Values (Brinell)	
AISI/SAE 1050	B ₀	No Heat Treatment	1	200	
			2	195	
			3	194	
	AVERAGE HARDNESS of B ₀				196
	B ₁	900°C/ 3h/ FC*	1	170	
			2	164	
			3	164	
	AVERAGE HARDNESS of B ₁				166
	B ₂	750°C/ 3h & 650°C/ 6h/FC*	1	177	
			2	172	
			3	170	
	AVERAGE HARDNESS of B ₂				173
	B ₃	900°C/ 3h/ FC*	1	144	
			2	141	
			3	136	
	AVERAGE HARDNESS of B ₃				140

* Furnace Cooling

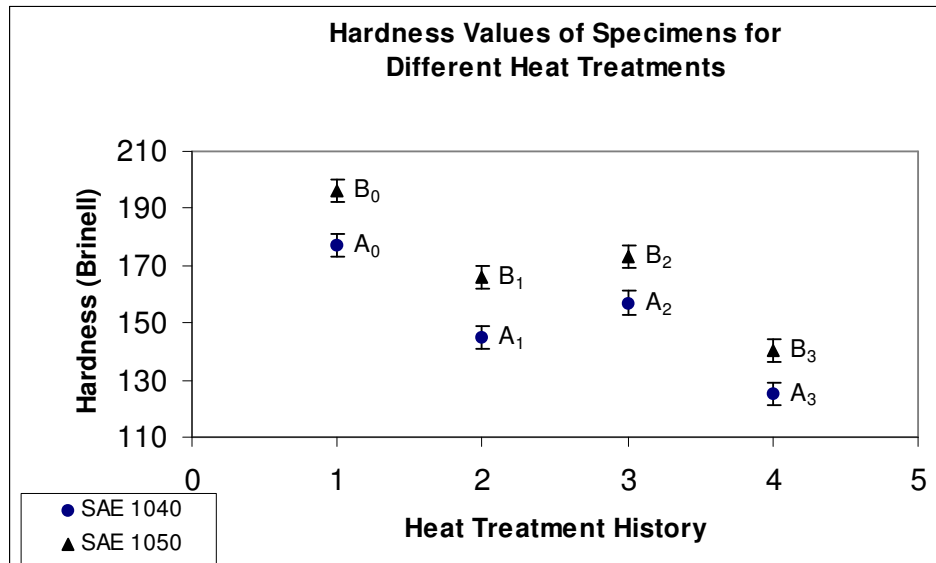


Figure 7.5: Hardness value changes of SAE 1040 and SAE 1050 specimens as a result of applied heat treatments

By looking at the hardness values, it can be said that for both steel types, maximum hardness values belongs to the non-heat treated specimens and all the applied heat treatments decrease the hardness values. As expected, hardness of the SAE 1050 is more than SAE 1040 and this shows that carbon is the major element that effects hardness and as carbon content increases, hardness increases.

For the second heat treatment group, that has 900°C/3h- furnace cooling treatment, it is seen that hardness values are lower than the non-heat treated specimens. Hardness values of second group are very close to the third group and only 7-8 Brinell less than the third group specimens. It is a known fact that annealing treatment decreases hardness and these results are parallel to that statement.

For the third heat treatment group, that has 750°C/3h-650°C/6h-furnace cooling treatment, it is seen that hardness values are lower than the non-heat treated specimens, very close to the second group of specimens, and higher than the fourth group of specimens. Since waiting time in the furnace is not as long as the fourth

group, excessive decarburization has not taken place and hardness values do not drop to much lower values.

For both steel types, lowest hardness values are achieved with treatment of 700°C/72h. This is an expected result thus, as structure turns to spherodite, hardness decreases and ductility increases. Since steel specimens waited for long times in the furnace, decarburization occurs and as a result of decrease in the carbon content, hardness decrease takes place.

7.4 Results of the Ultrasonic Wave Velocity Measurements

Table 7.4: Ultrasonic wave velocities of SAE 1040 specimens
(measured with 5 MHz straight beam probe)

SAE 1040 Steel Specimen Code A₀	Specimen Number	Time (μs)	Specimen Thickness (mm)	Sound Velocity (m/s)
	1	3.215	9.61	5980
	2	3.216	9.60	5971
	3	3.218	9.60	5966
	4	3.222	9.59	5953
	Average	3.218	9.60	5967
	Standard Deviation	-		10.90
SAE 1040 Steel Specimen Code A₁	Specimen Number	Time (μs)	Specimen Thickness (mm)	Sound Velocity (m/s)
	1	3.232	9.61	5945
	2	3.217	9.60	5969
	3	3.207	9.59	5981
	4	3.198	9.60	6004
	Average	3.213	9.60	5975
	Standard Deviation	-		24.18

Table 7.4: Continued

SAE 1040 Steel Specimen Code A ₂	Specimen Number	Time (μ s)	Specimen Thickness (mm)	Sound Velocity (m/s)
	1	3.221	9.59	5955
	2	3.217	9.60	5968
	3	3.207	9.60	5987
	4	3.215	9.60	5972
	Average	3.215	9.60	5971
	Standard Deviation	-		12.76
SAE 1040 Steel Specimen Code A ₃	Specimen Number	Time (μ s)	Specimen Thickness (mm)	Sound Velocity (m/s)
	1	3.170	9.60	6056
	2	3.195	9.61	6015
	3	3.186	9.60	6027
	4	3.174	9.59	6043
	Average	3.181	9.60	6035
	Standard Deviation	-		18.13

Table 7.5: Ultrasonic wave velocities of SAE 1050 specimens
(measured with 5 MHz straight beam probe)

SAE 1050 Steel Specimen Code B ₀	Specimen Number	Time (μ s)	Specimen Thickness (mm)	Sound Velocity (m/s)
	1	3.224	9.60	5956
	2	3.214	9.61	5981
	3	3.215	9.59	5965
	4	3.203	9.59	5988
	Average	3.214	9.60	5973
	Standard Deviation	-		14.81

Table 7.5: Continued

SAE 1050 Steel Specimen Code B₁	Specimen Number	Time (μ s)	Specimen Thickness (mm)	Sound Velocity (m/s)
	1	3.205	9.59	5984
	2	3.207	9.59	5981
	3	3.204	9.61	5999
	4	3.202	9.60	5997
	Average	3.205	9.60	5990
	Standard Deviation	-		8.76
SAE 1050 Steel Specimen Code B₂	Specimen Number	Time (μ s)	Specimen Thickness (mm)	Sound Velocity (m/s)
	1	3.199	9.59	5995
	2	3.206	9.58	5976
	3	3.204	9.61	5997
	4	3.206	9.61	5995
	Average	3.204	9.60	5991
	Standard Deviation	-		10.09
SAE 1050 Steel Specimen Code B₃	Specimen Number	Time (μ s)	Specimen Thickness (mm)	Sound Velocity (m/s)
	1	3.188	9.58	6011
	2	3.169	9.61	6065
	3	3.175	9.61	6054
	4	3.181	9.60	6036
	Average	3.178	9.60	6041
	Standard Deviation	-		23.84

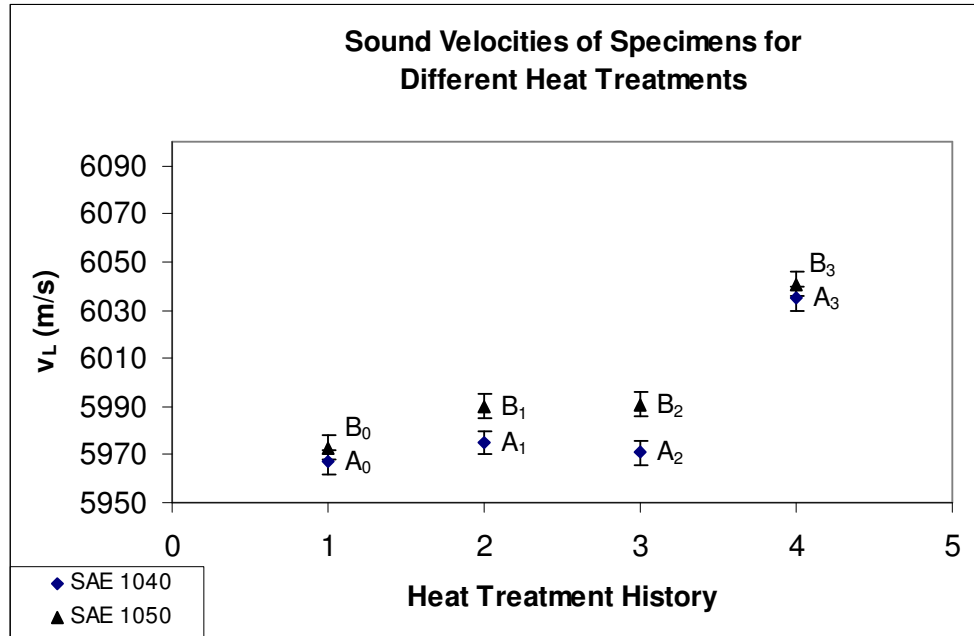


Figure 7.6: Sound velocity results of SAE 1040 and SAE 1050 specimens (measured with 5 MHz straight beam probe)

For the case of SAE 1040 specimen velocity measurement with 5 MHz straight beam probe, it can be seen that lowest sound velocity belongs to the non-heat treated specimen and highest sound velocity belongs to the specimen that has treatment of 700°C/72h. Velocity difference is very obvious for this specimen with respect to other specimens. As stated, lowest sound velocity belongs to the non-heat treated specimen however, since sound velocity results of first three group specimens are very close to each other and it is not possible to make a definite statement about their sound velocity change behaviours, by taking into account the error limits.

For the case of SAE 1050 specimens, it is seen that similar to the sound velocity results of SAE 1040 specimens with 5 MHz longitudinal probe, specimen having no heat treatment has lowest, and specimen having 700°C/72h treatment has the highest sound velocity. Although SAE 1050 specimens have higher carbon content and thus higher hardness, their sound velocities slightly higher than the SAE 1040

specimens and this shows that directional property of materials also plays a role on affecting sound velocity.

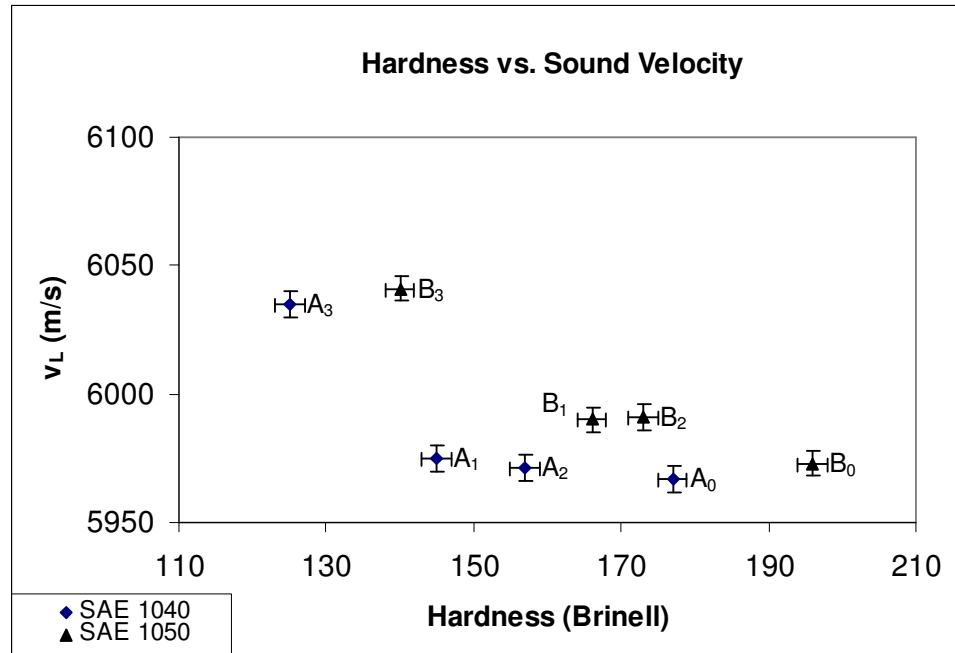


Figure 7.7: Hardness vs. sound velocity results of specimens (measured with 5 MHz straight beam probe)

As can be seen from Figure 7.7, sound velocity is the maximum for SAE 1040 specimen with lowest hardness and lowest for the specimen with highest hardness and an inverse relationship between hardness and sound velocity is observed. However, it must be taken into account that, values for the first three specimen groups are very close to each other and their sound velocity value differences are within the error limits.

Figure 7.7 also shows that hardness and sound velocity has a general inverse relationship for SAE 1050 steels as in the case of SAE 1040 specimens. Specimen having lowest hardness has highest sound velocity and specimen having highest hardness has lowest sound velocity. Again, similar to the case of SAE 1040

specimens, second and third group specimens having very close sound velocity values but as can be seen their hardness values are very close to each other.

Table 7.6: Ultrasonic wave velocities of SAE 1040 specimens
(measured with 10 MHz straight beam probe)

SAE 1040 Steel Specimen Code A₀	Specimen Number	Time (μ s)	Specimen Thickness (mm)	Sound Velocity (m/s)
	1	3.227	9.61	5956
	2	3.216	9.60	5971
	3	3.208	9.60	5985
	4	3.209	9.59	5977
	Average	3.215	9.60	5972
	Standard Deviation	-		12.30
SAE 1040 Steel Specimen Code A₁	Specimen Number	Time (μ s)	Specimen Thickness (mm)	Sound Velocity (m/s)
	1	3.208	9.61	5992
	2	3.217	9.60	5969
	3	3.211	9.59	5973
	4	3.205	9.60	5992
	Average	3.210	9.60	5981
	Standard Deviation	-		11.95
SAE 1040 Steel Specimen Code A₂	Specimen Number	Time (μ s)	Specimen Thickness (mm)	Sound Velocity (m/s)
	1	3.202	9.59	5990
	2	3.223	9.60	5959
	3	3.216	9.60	5970
	4	3.212	9.60	5978
	Average	3.213	9.60	5974
	Standard Deviation	-		13.47

Table 7.6: Continued

SAE 1040 Steel Specimen Code A ₃	Specimen Number	Time (μ s)	Specimen Thickness (mm)	Sound Velocity (m/s)
	1	3.186	9.60	6026
	2	3.177	9.61	6050
	3	3.192	9.60	6014
	4	3.158	9.59	6073
	Average	3.178	9.60	6041
	Standard Deviation	-		25.86

Table 7.7: Ultrasonic wave velocities of SAE 1050 specimens
(measured with 10 MHz straight beam probe)

SAE 1050 Steel Specimen Code B ₀	Specimen Number	Time (μ s)	Specimen Thickness (mm)	Sound Velocity (m/s)
	1	3.224	9.60	5956
	2	3.208	9.61	5991
	3	3.215	9.59	5966
	4	3.199	9.59	5996
	Average	3.212	9.60	5977
	Standard Deviation	-		19.68
SAE 1050 Steel Specimen Code B ₁	Specimen Number	Time (μ s)	Specimen Thickness (mm)	Sound Velocity (m/s)
	1	3.199	9.59	5995
	2	3.213	9.59	5969
	3	3.217	9.61	5976
	4	3.206	9.60	5989
	Average	3.209	9.60	5982
	Standard Deviation	-		12.05

Table 7.7: Continued

SAE 1050 Steel Specimen Code B₂	Specimen Number	Time (μ s)	Specimen Thickness (mm)	Sound Velocity (m/s)
	1	3.199	9.59	5995
	2	3.207	9.58	5974
	3	3.214	9.61	5980
	4	3.204	9.61	5998
	Average	3.206	9.60	5987
	Standard Deviation	-		11.22
SAE 1050 Steel Specimen Code B₃	Specimen Number	Time (μ s)	Specimen Thickness (mm)	Sound Velocity (m/s)
	1	3.144	9.58	6095
	2	3.168	9.61	6066
	3	3.181	9.61	6041
	4	3.153	9.60	6090
	Average	3.161	9.60	6073
	Standard Deviation	-		24.37

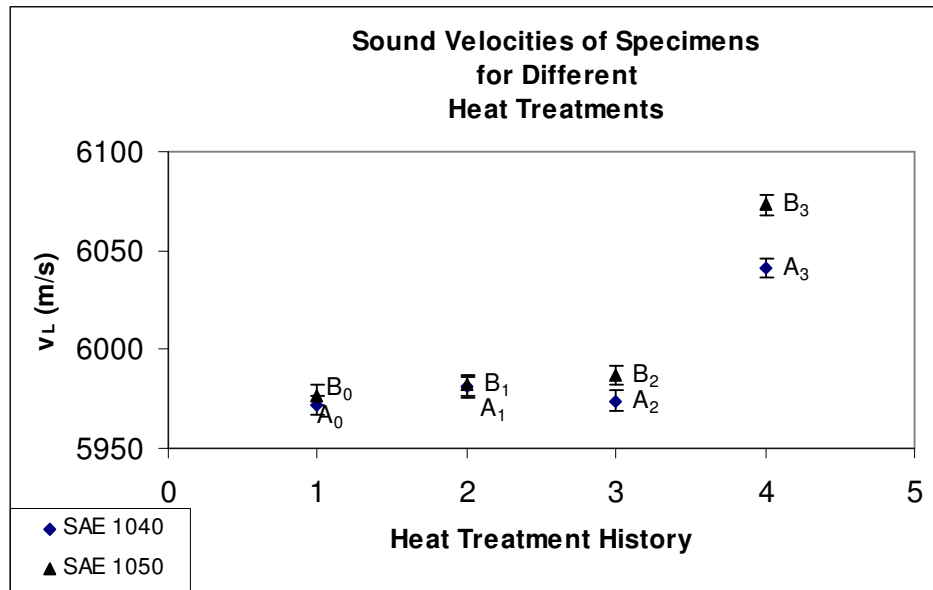


Figure 7.8: Sound velocity results of SAE 1040 and SAE 1050 specimens (measured with 10 MHz longitudinal probe)

For the measurement of SAE 1040 specimens with 10 MHz straight beam probes, similar results are achieved to the measurements of 5 MHz straight beam probe. The highest sound velocity belongs to the specimen that has treatment of 700°C/72h and specimen that is not heat treated has the lowest sound velocity. Sound velocity values of the first three specimens are again very close to each other.

For the case of velocity measurement of SAE 1050 specimens with 10 MHz straight beam probe, a similar results with the 5 MHz straight beam probes obtained. Non-heat treated specimen has lowest, and 700°C/72h heat treated specimen has the highest sound velocity. Again similar to the previous cases, first three group of specimens have very close sound velocity values.

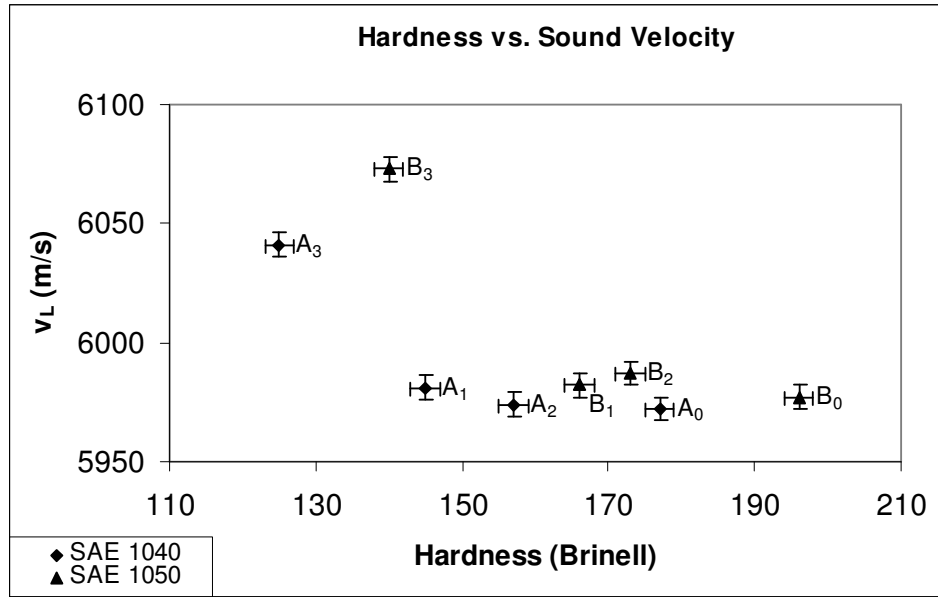


Figure 7.9: Hardness vs. sound velocity results of specimens (measured with 10 MHz straight beam probe)

For SAE 1040 specimens- sound velocity change with respect to hardness values follows again a general inverse relationship similar to the case of 5 MHz straight beam probe measurements. Specimen having lowest hardness has the highest sound velocity and specimen having highest hardness has lowest sound velocity. For the first three group of specimens, sound velocity values are very close to each other.

A general inverse relationship between hardness and sound velocity is observed for sound velocities of SAE 1050 specimens measured with 10 MHz straight beam probe. Second and third group specimens has very close hardness values and their velocity difference is within the error limits. Again, specimen having lowest hardness has highest sound velocity and specimen having highest hardness has lowest sound velocity.

Table 7.8: Ultrasonic wave velocities of SAE 1040 specimens
(measured with 5 MHz shear wave probe)

SAE 1040 Steel Specimen Code A₀	Specimen Number	Time (μ s)	Specimen Thickness (mm)	Sound Velocity (m/s)
	1	5.932	9.61	3240
	2	5.915	9.60	3247
	3	5.899	9.60	3255
	4	5.900	9.59	3251
	Average	5.911	9.60	3248
	Standard Deviation	-		6.48
SAE 1040 Steel Specimen Code A₁	Specimen Number	Time (μ s)	Specimen Thickness (mm)	Sound Velocity (m/s)
	1	5.934	9.61	3239
	2	5.908	9.60	3251
	3	5.876	9.59	3264
	4	5.913	9.60	3247
	Average	5.908	9.60	3250
	Standard Deviation	-		10.42
SAE 1040 Steel Specimen Code A₂	Specimen Number	Time (μ s)	Specimen Thickness (mm)	Sound Velocity (m/s)
	1	5.916	9.59	3242
	2	5.908	9.60	3250
	3	5.891	9.60	3259
	4	5.902	9.60	3254
	Average	5.904	9.60	3251
	Standard Deviation	-		7.07

Table 7.8: Continued

SAE 1040 Steel Specimen Code A ₃	Specimen Number	Time (μ s)	Specimen Thickness (mm)	Sound Velocity (m/s)
	1	5.873	9.60	3269
	2	5.905	9.61	3255
	3	5.910	9.60	3248
	4	5.871	9.59	3267
	Average	5.890	9.60	3260
	Standard Deviation	-		9.59

Table 7.9: Ultrasonic wave velocities of SAE 1050 specimens
(measured with 5 MHz shear wave probe)

SAE 1050 Steel Specimen Code B ₀	Specimen Number	Time (μ s)	Specimen Thickness (mm)	Sound Velocity (m/s)
	1	5.893	9.60	3258
	2	5.921	9.61	3247
	3	5.922	9.59	3239
	4	5.896	9.59	3253
	Average	5.908	9.60	3249
	Standard Deviation	-		8.28
SAE 1050 Steel Specimen Code B ₁	Specimen Number	Time (μ s)	Specimen Thickness (mm)	Sound Velocity (m/s)
	1	5.885	9.59	3259
	2	5.920	9.59	3241
	3	5.914	9.61	3250
	4	5.895	9.60	3257
	Average	5.903	9.60	3251
	Standard Deviation	-		8.58

Table 7.9: Continued

SAE 1050 Steel Specimen Code B₂	Specimen Number	Time (μ s)	Specimen Thickness (mm)	Sound Velocity (m/s)
	1	5.903	9.59	3249
	2	5.879	9.58	3259
	3	5.899	9.61	3258
	4	5.914	9.61	3251
	Average	5.899	9.60	3254
	Standard Deviation	-		5.23
SAE 1050 Steel Specimen Code B₃	Specimen Number	Time (μ s)	Specimen Thickness (mm)	Sound Velocity (m/s)
	1	5.730	9.58	3344
	2	5.784	9.61	3323
	3	5.770	9.61	3332
	4	5.780	9.60	3322
	Average	5.766	9.60	3330
	Standard Deviation	-		10.16

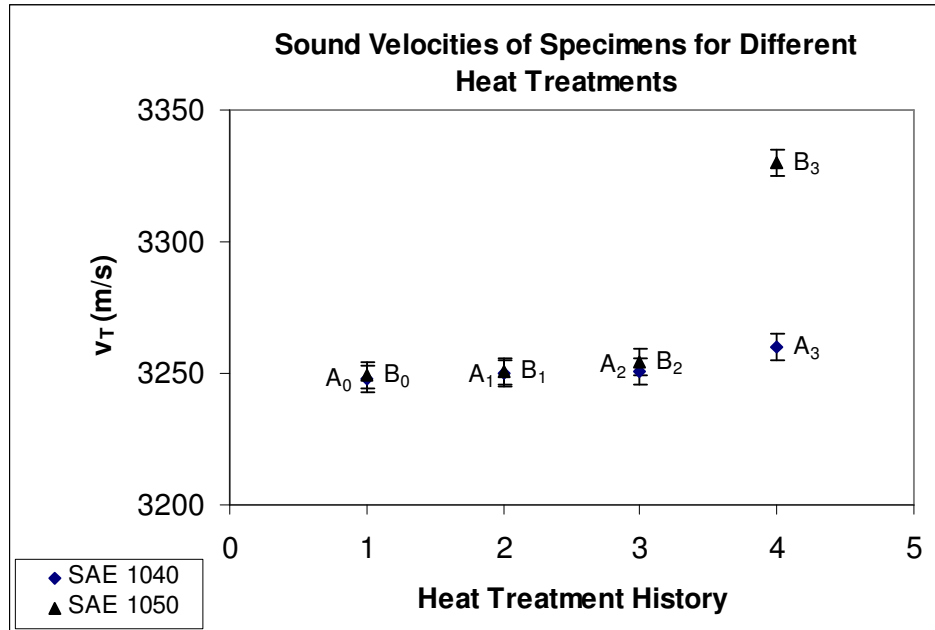


Figure 7.10: Sound velocity results of SAE 1040 and SAE 1050 specimens (measured with 5 MHz shear wave probe)

On the measurement of SAE 1040 specimens with 5 MHz shear wave probe, same behaviour as the measurements of 5 and 10 MHz straight beam probes is observed but in this case all the measurements are very close to each other and a distinct difference of fourth group of specimens with respect to others is not observed as the case of measurement with straight beam probes. Specimen having highest sound velocity belongs to that has treatment of 700°C/72h and lowest velocity belongs to the specimen of non-heat treated specimen. By looking to the measurement results of the three probe types, it can be said that, generally similar sound velocity characteristics are observed.

For the case of measurement of the SAE 1050 specimens with 5 MHz shear wave probes, similar behaviour of the sound velocity results are observed to the previous measurements. Non-heat treated specimen has lowest and 700°C/72h heat treated specimen has the highest sound velocity.

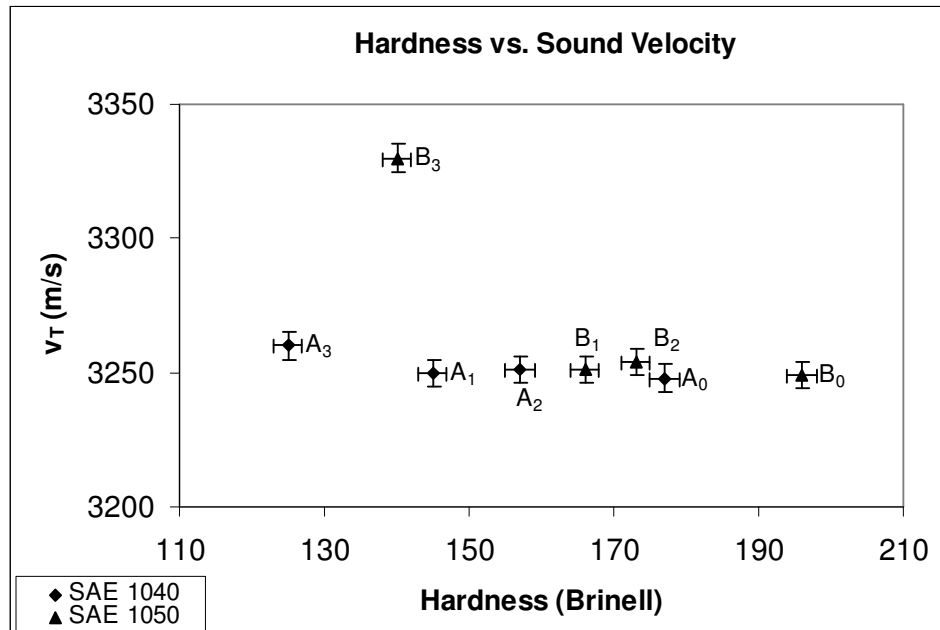


Figure 7.11: Hardness vs. sound velocity results of specimens (measured with 5 MHz shear wave probe)

For SAE 1040 specimens, hardness and sound velocity relationship is again similar to the measurements made with straight beam probes, but since sound velocity values are very close to each other, a distinct inverse relationship between sound velocity and hardness values can not be observed.

For SAE 1050 specimens, a general inverse relationship between hardness and sound velocity is also generally observed. Specimen having lowest hardness value has highest and specimen having highest hardness has lowest sound velocity. As in the previous cases, second and third group of specimens have very close hardness and sound velocity values.

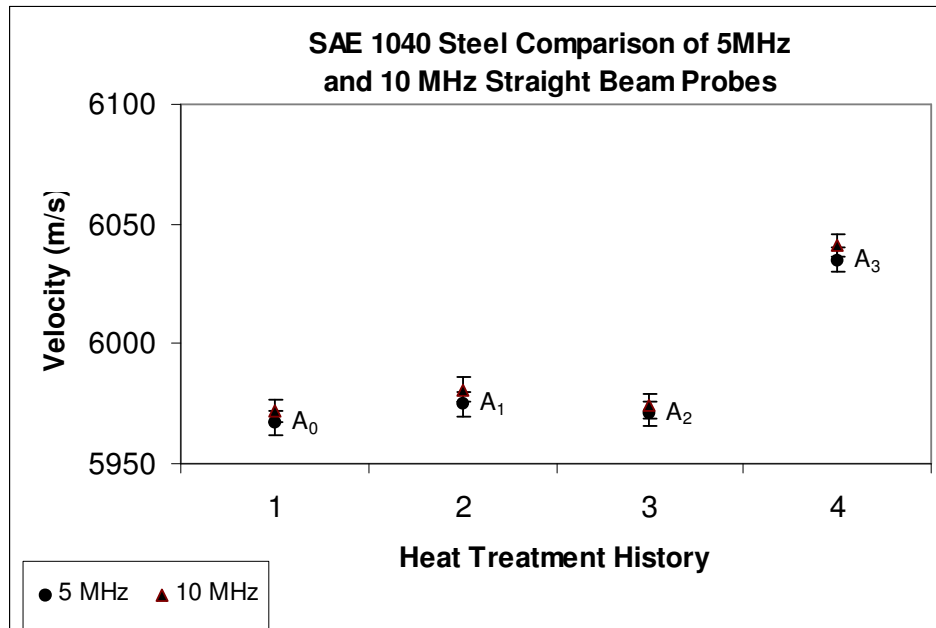


Figure 7.12: Comparison of velocity measurements of SAE 1040 steels with 5MHz and 10 MHz straight beam probes

Comparison of the measurements made with 5 and 10 MHz straight beam probes shows that results are very close to each other and it can be concluded that frequency of the probe has a very little effect on the sound velocity measurement.

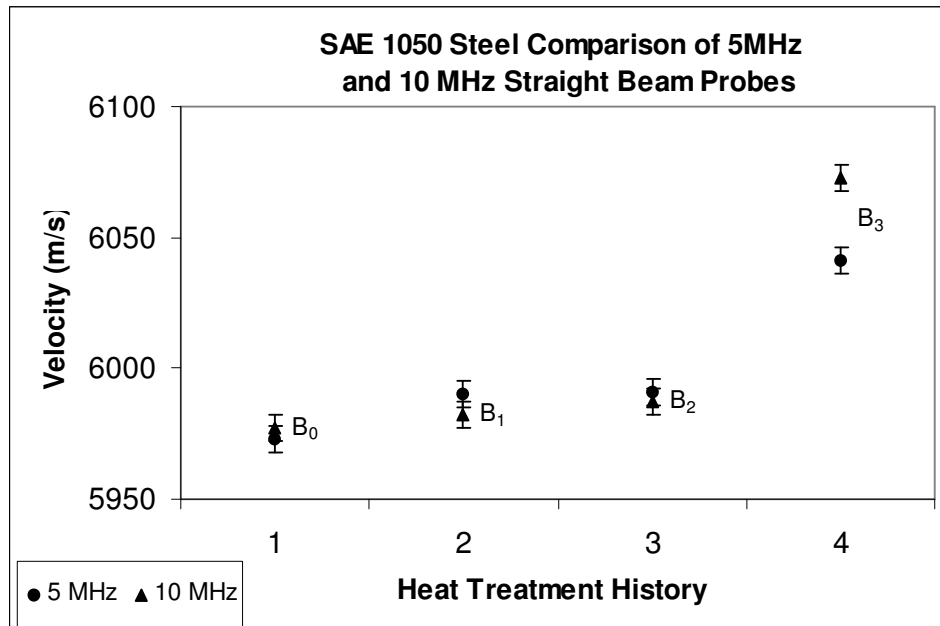


Figure 7.13: Comparison of velocity measurements of SAE 1050 steel with 5MHz and 10 MHz straight beam probes

Figure 7.13 shows that, results obtained with 5 and 10 MHz straight beam probes are very close to each other. Only for the fourth group, a small difference present. From this result, it can again be concluded that frequency of the probe has a very little effect on the sound velocity measurement.

7.5 Results of the Tool Life Tests

Table 7.10: Flank wear land measurement results of the SAE 1040 specimens

Cutting Velocity V= 53.72 m/min					Cutting Velocity V= 65.36 m/min				
Cutting Time (min)	Flank Wear Land (mm)				Cutting Time (min)	Flank Wear Land (mm)			
	A ₀	A ₁	A ₂	A ₃		A ₀	A ₁	A ₂	A ₃
4	0.111	0.085	0.067	0.091	2	0.195	0.152	0.149	0.161
8	0.151	0.128	0.101	0.122	4	0.223	0.181	0.174	0.189
12	0.167	0.149	0.118	0.140	6	0.239	0.194	0.189	0.201
16	0.181	0.164	0.129	0.157	8	0.254	0.205	0.201	0.213
20	0.193	0.178	0.137	0.169	10	0.308	0.218	0.214	0.225
24	0.212	0.191	0.150	0.183	12		0.232	0.227	0.241
28	0.258	0.207	0.162	0.198	14		0.244	0.239	0.259
32	0.309	0.220	0.184	0.211	16		0.275	0.251	0.308
36		0.242	0.196	0.245	18		0.309	0.263	
40		0.284	0.215	0.293	20			0.305	
44		0.335	0.255		22				
48			0.305		24				

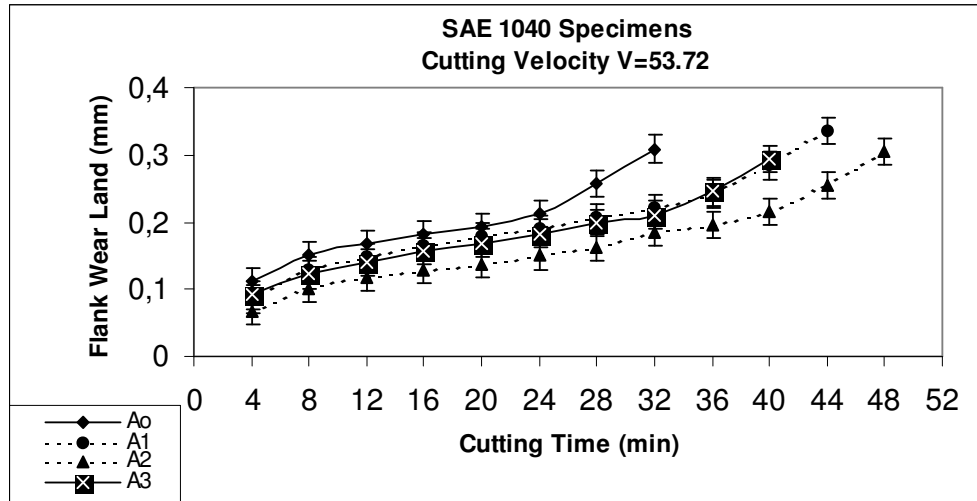


Figure 7.14: Flank wear land measurements of SAE 1040 specimens for cutting velocity $V=53.72$ m/min

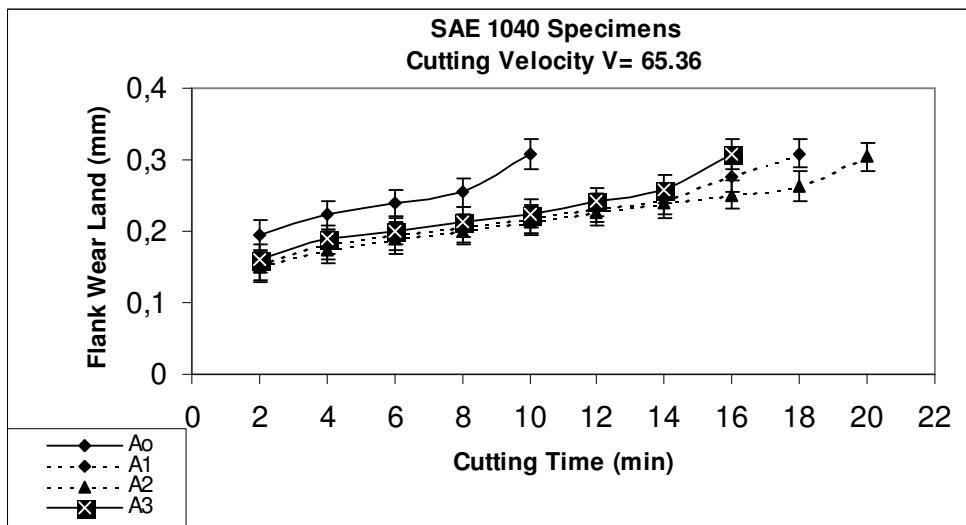


Figure 7.15: Flank wear land measurements of SAE 1040 specimens for cutting velocity $V=65.36$ m/min

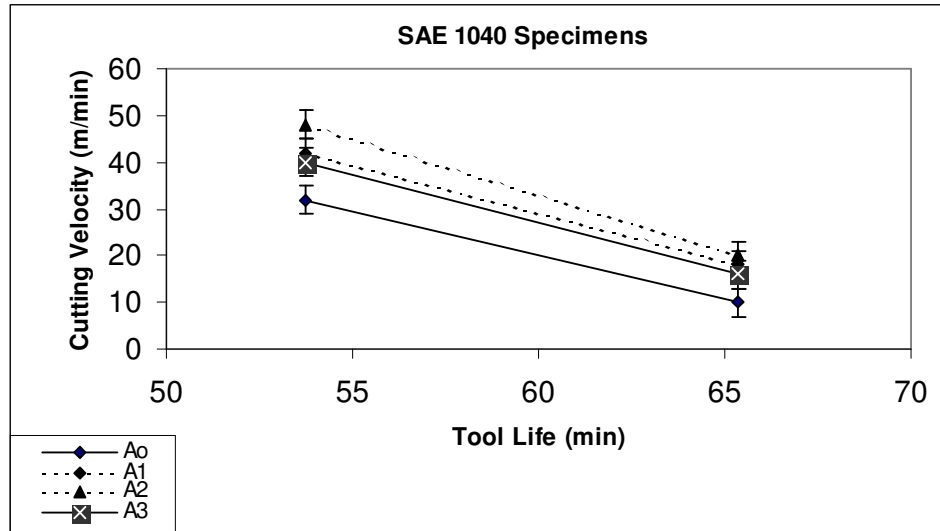


Figure 7.16: Tool life vs. cutting velocity curves for SAE 1040 specimens

For the case of tool life tests of SAE 1040 specimens with $V=53.72$ m/min cutting velocity, it can be seen that the longest tool life is achieved with A_2 specimen which has heat treatment of $750^{\circ}\text{C}/3\text{h}-650^{\circ}\text{C}/6\text{h}$ - furnace cooling. The second best tool life result is achieved with A_1 specimen that has heat treatment of $900^{\circ}\text{C}/3\text{h}$ -furnace cooling. A_3 specimen which has heat treatment of $700^{\circ}\text{C}/72\text{h}$ - furnace cooling has better tool life result than non-heat treated specimen but worse than the specimens A_1 and A_2 . All the applied heat treatments have increased the tool life at some extent.

Table 7.11: Flank wear measurement results of the SAE 1050 specimens

Cutting Velocity V= 53.72 m/min					Cutting Velocity V= 65.36 m/min				
Cutting Time (min)	Flank Wear Land (mm)				Cutting Time (min)	Flank Wear Land (mm)			
	B ₀	B ₁	B ₂	B ₃		B ₀	B ₁	B ₂	B ₃
4	0.175	0.147	0.137	0.148	2	0.234	0.182	0.173	0.177
8	0.209	0.182	0.175	0.177	4	0.254	0.215	0.204	0.209
12	0.222	0.197	0.191	0.195	6	0.293	0.231	0.219	0.226
16	0.243	0.203	0.204	0.202	8		0.245	0.233	0.241
20	0.296	0.225	0.218	0.221	10		0.263	0.246	0.255
24		0.244	0.235	0.242	12		0.304	0.261	0.272
28		0.286	0.249	0.259	14			0.309	0.319
32		0.331	0.278	0.281	16				
36			0.309	0.326	18				

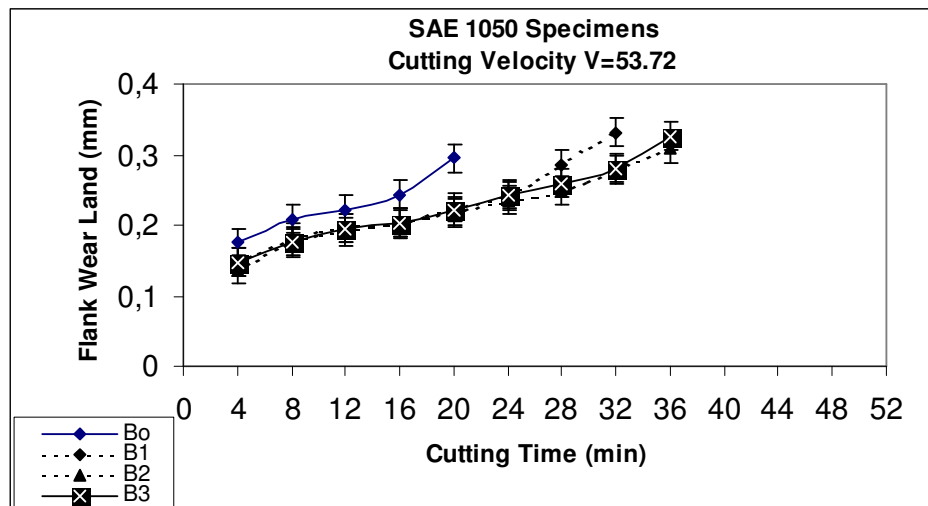


Figure 7.17: Flank wear land measurements of SAE 1050 specimens for cutting velocity V=53.72 m/min

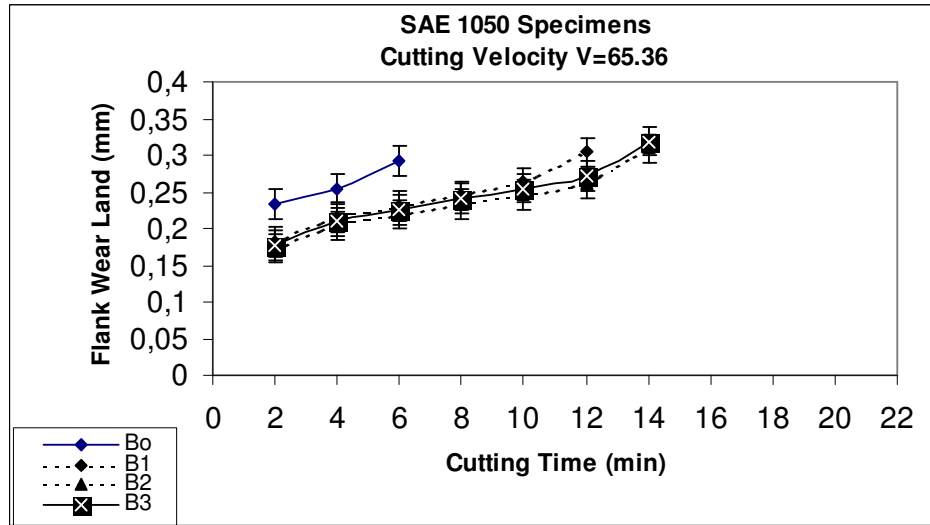


Figure 7.18: Flank wear land measurements of SAE 1050 specimens for cutting velocity $V=65.36$ m/min

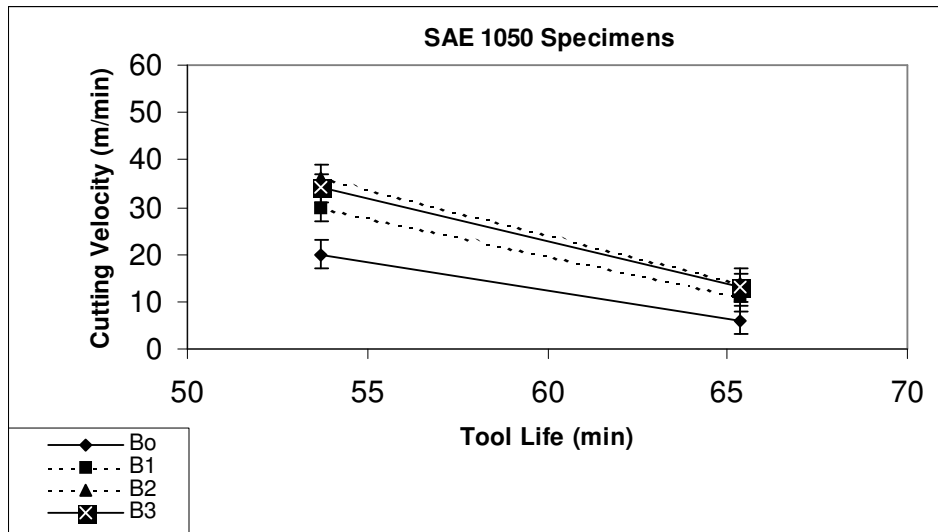


Figure 7.19 : Tool life vs. cutting velocity curves for SAE 1050 specimens

For the case of tool life tests of SAE 1050 specimens with $V=53.72$ m/min cutting velocity, it can be seen that the longest tool life is achieved with B_2 specimen which has heat treatment of $750^{\circ}\text{C}/3\text{h}-650^{\circ}\text{C}/6\text{h}$ - furnace cooling. The second best tool

life result is achieved with B₃ specimen that has heat treatment of 700°C/72h-furnace cooling. B₁ specimen which has heat treatment of 900°C/3h- furnace cooling has better tool life result than non-heat treated specimen but worse than the specimens B₂ and B₃. All the applied heat treatments have increased the tool life at some extent.

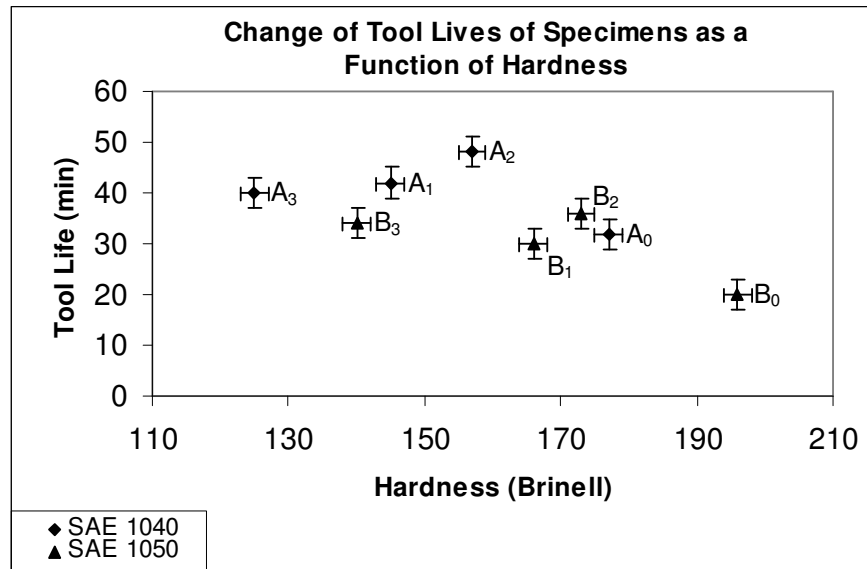


Figure 7.20: Change of tool lives of specimens at V=53.72 m/min cutting velocity as a function of hardness

For the case of SAE 1040 specimens, it can be concluded that tool life and hardness has not a linear relation. From the hardness value of 125 HB to the 157 HB tool life increases with increasing hardness, but when hardness value exceeds to 177 HB, tool life reduces.

For SAE 1050 specimens, as in the case of SAE 1040 specimens, it can be concluded that tool life and hardness has not a linear relation. The worst tool life result is achieved with the non-heat treated specimens that has highest hardness. Specimen having hardness value of 173 HB has the best tool life.

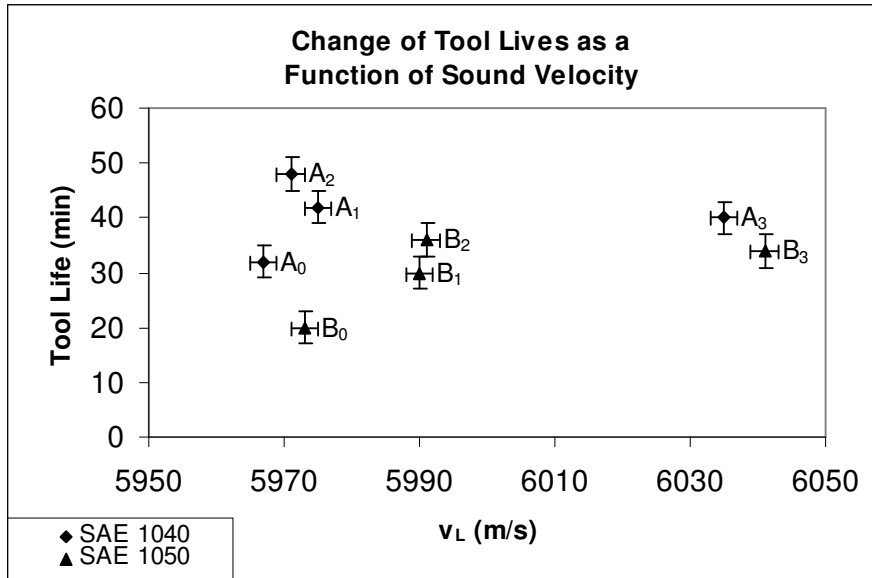


Figure 7.21: Change of tool lives of specimens at $V=53.72$ m/min cutting velocity as a function of sound velocity (measured with 5 MHz straight beam probe)

As can be seen from Figure 7.21, it is not possible to make a correlation between sound velocity and tool life test results.

7.6 Discussion

All the heat treatments applied in this study, have decreased the hardness and sound velocity values. In the previous studies [37, 41], it was concluded that hardness and ultrasonic sound velocity has a general inverse relationship which are also parallel to the results achieved in this study. Applied heat treatments increased the grain size of the specimens and thus led to an increase in the sound velocities. Previous studies performed on ultrasonic velocity and microstructure relationship shows that ultrasonic velocity affected by grain size and microstructure. Vasudevan et al., in their study found that an increase in grain boundary area, which means decrease in grain size, results in large scattering of ultrasonic waves which causes

ultrasonic waves to take a longer path to cover the material thickness, which decreases the ultrasonic velocity drastically [8].

As in the case of fourth group, decrease in hardness and increase in sound velocity values is very obvious. For the rest of the specimens, this change is not so significant as the fourth group but it must be taken into account that, second and third group of specimens have very close hardness values and it is normal to have close sound velocity values within the error limits. When comparing sound velocities of SAE 1040 and 1050 samples, it is seen that SAE 1050 samples have higher sound velocity values than SAE 1040 steels although they have higher hardness values. This shows that, directional property of materials also plays a role on affecting sound velocity as well as hardness.

It has been previously reported that an increase in the dislocation density decreases the ultrasonic velocity. Prasad and Kumar [7] concluded that ultrasonic velocity decreases with the increase in the degree of deformation on the material, and this decrease is only due to the increase in dislocation density. Since it is a known fact that, all the applied treatments in this study leads to a decrease in the dislocation density, increase in the ultrasonic sound velocity values as a result of applied heat treatments is an expected result.

By looking at Figures 7.12 and 7.13, it can be concluded that measured longitudinal velocities with 5 and 10 MHz probes are nearly the same. Occurrence of small differences can be explained by frequency dependence of velocity due to dispersion. From this, it can be concluded that ultrasonic sound velocity is not frequency dependent. As stated in previous studies [37, 42], dispersive character can be due to instrumentation, bonding and due to material itself. Since the used probes were not identical, dispersion could be the result for these differences.

On performing the tool life tests, in order to avoid the variation of the results due to the differences in the test conditions, ISO 3685:1993 E Tool Life Testing with Single-Point Tools Standard procedures were followed as far as possible. Although,

test conditions were arranged according to the standard, there were still possible error sources due to various reasons. One important point need to be considered is that, used engine lathe was very old and it likely to have some vibrations when operating. Other important point is that, tool wear measurements were performed by eye judgement and it is likely to have small variations in the tool wear measurements. In order to minimize the error, each measurement was made three times.

In tool life tests major disadvantage is that, they are very time, material and energy consuming tests and repeatability of these tests is not possible. As mentioned before, when same test is performed with another engine lathe, it is not surprising to have different results. In the case of this study, with some unavoidable error, parallel results to the previous studies are achieved.

Shaw [43], states that, wear land values that have been measured directly, using a tool maker's microscope, have shown a resulting data with considerable scatter indicating a large amount of uncertainty in the measurements, and therefore he concluded that this scatter might be attributed to the variation of the wear land across the tool, which in turn leads to difficulties in determining the exact extent of the wear land. However, since these variations are inherent to almost all tool life tests, and since the results recorded for a set of tests that are statistical in nature, there still remains the possibility of a comparison between such results.

The purpose of this study was the investigation of the change in machinability properties of medium carbon steels as a result of spherodizing and also annealing treatment. Achieved results have showed that there is a relation between metallurgical conditions of the workpieces and machinability properties. It can be concluded from these results that, hardness and microstructure of the workpiece together plays an important role on machinability properties. From these results, it can also be concluded that there is an optimum hardness range for best machinability conditions and higher and lower hardness values than this range

results with the decrease in machinability characteristics. This result is parallel to the statements presented in the references.

Parallel to the conclusion which can be made from this study, Tipi [44] has observed that cutting velocity has a significant effect on the tool life. Small increase in the cutting velocity resulted with dramatic decrease in the tool life. In the same study, it was also observed that hardness of the workpiece has an effect on machinability results and when hardness value is higher than the optimum values, tool life decreases as in the case of this study.

Parallel to the conclusions which can be made from this study, it has been observed by Kronenberg [45] that, steels with small amounts of pearlite exhibit either longer tool life or higher permissible cutting speeds. It has been shown that tool life decreases as carbon content increases. In another study performed by Araki [46], it has been reported that, harder specimens caused tool failure in a short time than the softer specimens. Other study performed by Armarego, and Brown [47] also confirms these theories and achieved similar results.

As an auxillary study, ultrasonic sound velocity changes as a result of applied treatments also investigated and it has been observed that it is not likely to have a direct correlation between ultrasonic sound velocity and machinability properties.

CHAPTER VIII

CONCLUSION

This thesis was conducted to investigate the effect of metallurgical properties of the workpieces on the machinability characteristics of the steels. For this purpose two medium carbon steel types namely AISI/SAE 1040 and 1050 were used and each steel type was divided into four categories. One group was left as reference group and no heat treatment was performed on them. Other steels have experienced three different heat treatments. After these studies their microstructural analysis, hardness measurements, ultrasonic wave velocity measurements were performed on representative specimens. As a last step, tool life tests were performed on these workpieces on an engine lathe. With all the results that were achieved from this study, following conclusions can be made:

- Heat treatments applied in this study affected the hardness values of the steels. In the case of 700°C/72h/furnace cooling treatment, this decrease is the most significant and material hardness value drops from 177 HB to 125 HB for SAE 1040 steels, and from 196 HB to 140 HB for SAE 1050 steels. For the case of other two heat treatments hardness decrease is also observed. So, it can be concluded that heat treatment has a great effect on hardness value of metals.
- Hardness values also show that carbon is the major element that affects the hardness of steels and as carbon content increases hardness of the steel increases. Microstructural photographs also show that as carbon content increases, amount of pearlite in the steel increases.

- By looking at the results obtained with longitudinal and transverse waves, it can be concluded that longitudinal and transverse waves behave in a similar manner for similar steel microstructures.
- Comparison of the 5 and 10 MHz longitudinal probes shows that results are very close to each other and it can be concluded that frequency of the probe has a very little effect on the sound velocity measurement between 5-10 MHz range.
- By looking at the experimental results it can be concluded that, applied heat treatments also affect the ultrasonic velocities. Ultrasonic wave velocity is maximum for non-heat treated steels for both SAE 1040 and 1050, and as a result of applied heat treatments ultrasonic wave velocities increased. In the case of 700°C/72h/furnace cooling heat treatment, this increase is maximum for both steel types. Other applied two treatments also increased the sound velocity values.
- When comparing the hardness values with ultrasonic wave velocities, an inverse relation is observed. As hardness of the specimens decreases, their ultrasonic wave velocity values increases.
- By looking at the results of the tool life tests, it can be concluded that hardness and microstructure of the workpiece together plays an important role on machinability properties. All the applied heat treatments have changed the machinability characteristics of the workpieces in some extent.
- For the selected medium carbon steels, the best machinability result was achieved with the steels having a microstructure of lamellar pearlite and spheroidite mixture. Completely spheroidized microstructures and annealed structures also gives better machinability results than the specimens in the non-heat treated condition.

- From the results, it can also be concluded that there is an optimum hardness range for best machinability conditions and higher and lower hardness values than this range results with the decrease in machinability characteristics. For the low hardness values, increasing ductility and built-up edge formation negatively affect the machinability characteristics, thus it decreases tool life. Above the optimum hardness range, increasing hardness also negatively affects the machinability, thus as material gets harder tool wears out more easily.

- Experimental results show that cutting velocity has a significant effect on the tool life. Small increase in the cutting velocity results with dramatic decrease in the tool life.

To conclude, the effect of microstructure on the ultrasonic wave velocity and machinability properties is an important subject and further investigations must be made with different samples and heat treatment types.

REFERENCES

- 1) Boothroyd, G., "Fundamentals of Metal Machining and Machine Tools", Central Book Company
- 2) Hull, J.B., John, V., "Non Destructive Testing", 1988, English Language Book Society/Macmillan
- 3) Papadakis E. P., "Ultrasonic Attenuation and Velocity in SAE 52100 Steel Quenched From Various Temperatures", Metallurgical Transactions, Volume 1, April, 1970, pp.1053-1057
- 4) Papadakis, E.P., "Physical Acoustics and Microstructure of Iron Alloys", International Metals Reviews, Vol.29, No.1, 1984, pp1-23.
- 5) Murav'ev, V. V., "Interrelationship of the Velocity of an Ultrasonic Wave in Steels and Their Heat Treat Cycles" Plenum Corporation, 1989, pp.135-137
- 6) Prasad, R., Kumar, S., "An Investigation into the Ultrasonic Behaviour of Cast and Heat-Treated Structures in Steel", British Journal of NDT, vol.33, No.10, 1991, pp.506-508.
- 7) Prasad, R., Kumar, S., "Study of the Influence of Deformation and Thermal Treatment on the Ultrasonic Behaviour of Steel", Journal of Materials Processing Technology, No 42, 1994, pp.51-59.

- 8) Vasudevan,E.,Palanichamy,P.,Venkadesan,S.,“A Novel Technique for Characterizing Annealing Behavior” Scripta Metallurgica et Materialia, vol.30, No.11,1994,pp.1479-1483
- 9) Palanichamy, P.Joseph A., Jayakumar T.,Raj B., “Influence of Grain Size on Ultrasonic Spectral Parameters in AISI Type 316 Stainless Steel”, Scripta Materialia, Vol.40, No.3, 1999, pp.333-340
- 10) Bouda,B.A., Benchaala.A., Alem,K., “Ultrasonic Characterization of Material Hardness”, Ultrasonics, Volume 38, March 2000, pp.: 224-227.
- 11) Bouda,A.B., Benchaala,A., Alem K., “Ultrasonic Characterization of Material Hardness”, Ultrasonics, No.38, 2000, pp.224-227
- 12) Palanichamy,P., Vasudevan, M., Jayakumar, T., Venugopal,S.,Raj,B., “Ultrasonic Velocity Measurements for Characterizing the Annealing Behaviour of Cold Worked Austenitic Stainless Steel”, NDT&E International, Vol.33,2000, pp.:253-259
- 13) Lim, C.H.Y., Lau,P.P.T., Lim,S.C., “The effects of work material on tool wear”, Wear, 2001, vol.250, pp.344-348
- 14) Ozcatalbas,Y., Ercan,F., “The effects of heat treatment on the machinability of mild steels”, Journal of Material Processing Technology, 2003, vol.136, pp.227- 238
- 15) Chou,Y.K., “Hard turning of M50 steel with different microstructures in continous and interminent cutting”, Wear, 2003, vol 255, pp. 1388-1394
- 16) Tekiner,Z., Yesilyurt,S., “Investigation of the cutting parameters depending on process sound during turning of AISI 304 austenitic stainless steel”, Materials & Design, 2003 vol.25, pp. 507-513

- 17) Korkut,I., Kasap,M.,Ciftci,I.,Seker,U., “Determination of optimum cutting parameters during machining of AISI 304 stainless steel”, *Materials&Design*, 2003, vol. 25, pp. 303-305
- 18) Sikdar, S.K., Chen,M., “Relationship between tool flank wear area and component forces in single point turning”, *Journal of Materials Processing Technology*, 2002 vol.128, pp. 210-215
- 19) Paro, J., Hanninen,H., Kauppinen,V., “Tool wear and machinability of x5CrMn 18 18 stainless steels”, *Journal of Materials Processing Technology*, 2001,vol.119, pp.14-20
- 20) Benga,G.C., Abrao, A.M., “Turning of hardened 100Cr6 bearing steel with ceramic and PCBN cutting tools”, *Journal of Materials Processing Technology*, 2003, vol. 143-144, pp. 237-241
- 21) Childs, T.H., Maekawa, K., Obikawa,T., Yamane, Y. “Metal Machining Theory and applications”, Arnold Publishers, 2000
- 22) Boulger,F.W.,“Machining Characteristics of Steels”,*Machinability (Proceedings of a Conference on Machinability)*, pp.565-585. London:Iron and Steel Institute, 1967.
- 23) Trent, E.M., “The Relationship Between Machinability and Tool Wear”, *Machinability (Proceedings of a Conference on Machinability)*, pp.179- 184. London:Iron and Steel Institute, 1967.
- 24) Mills, B., Redford, A.H., “Machinability of Engineering Materials”,*Applied Science Publishers*, 1983
- 25) ISO 3685:1993 Standard for Tool Life Testing with Single-Point Turning Tools

- 26) Taylor, F.W., "On the Art of Cutting Metals", Trans.ASME, vol.28,1906
- 27) Trent,E.M., "Metal Cutting", 3rd Edition, Butterworth Heinemeann,1991
- 28) Enahoro,H.E., Welsh,M.J.M., " The Relevance of the Mechanics of Metal Cutting to Machinability" (Proceedings of a Conference on Machinability), pp.179-184. London:Iron and Steel Institute,1967
- 29) Edwards, R. "Cutting Tools", London: Institute of Materials, 1993
- 30) Oxley, P.L.B., "Mechanics of Machining", John Wiley&Sons,1989
- 31) Lane, J.D., Stam, J.W., Wolfe, J.B., "General Introductory Review of the Relationship Between Metallurgy and Machinability", Machinability (Proceedings of a Conference on Machinability), pp.65-70. London:Iron and Steel Institute, 1967.
- 32) Barrett, C.R., Tetelman, A.S., "The Principles of Engineering Materials" Prentice-Hall, Inc.1973
- 33) John, V., "Introduction to Engineering Materials" Macmillan Education LTD,1992
- 34) ASTM Handbook Heat Treatment Vol 3
- 35) "Nondestructive Testing", .S. Atomic Energy Commission, Division of Technical
- 36) Sonat, M., "Ultrasonic Examination of Resistance Spot Welds", Ms.C Thesis, METU, January 1990.

- 37) Bozay C.V., "Correlation Between Ultrasonic Properties and Heat Treatment Conditions for Some Steels" Ms.C Thesis, METU, November 2002
- 38) Smith, A.L., "Ultrasonic Testing Fundamentals", Materials Evaluation, April, 1978, pp.:22-31
- 39) "ASM International, Metals Handbook", Nondestructive Evaluation and Quality Control, Vol.11, 9th edition, 1989
- 40) Green, B, "NDT Handbook", 1991, American Society for NDT
- 41) Keleş Y., "The Effect of Microstructure and Hardness on Acoustic Properties of Hypoeutectoid Plain-C Steels", Ms.C Thesis, METU, April 2002
- 42) Tuncer O., "Microstructural Characterization of Isothermally Heat Treated Steels by Ultrasonics", Ms.C Thesis, METU, August 2002
- 43) Shaw, M.C. "Principles of Metal Cutting", Massachusetts Institute of Technology
- 44) Tipi, C. "Investigation of Tool Life and Machinability Criteria in the Turning of Carbon Steels", MsC. Thesis, METU, January 1975
- 45) Kronenberg, M., "Machining Science and Application", Pergamon Press, 1966
- 46) Araki, T. "Some Results of Cooperative Research on the Effect of Heat Treated Structure on the Machinability of a Low Alloy Steel", American Society for Metals, 1975 pp: 381-395

- 47) Armarego, E.J.A., Brown,R.H., “The Machining of Metals,Prentice-Hall”,
1969
- 48) Krautkramer, J., Krautkramer, H., “ Ultrasonic Testing of Materials”,
Springer-Verlag, New York, 1983